Isolating climatic and paleomagnetic imbricated signals in two marine cores using principal component analysis

J.-P. Valet, E. Moreno, F. Bassinot, Ludger Johannes, F. Dewilde, T. Bastos, A. Lefort, M.-T. Venec-Peyre

Geochemistry Geophysics Geosystems G3

Article
Volume 12, Number 8
27 August 2011
Q08012, doi:10.1029/2011GC003697
ISSN: 1525-2027

Published by AGU and the Geochemical Society

Isolating climatic and paleomagnetic imbricated signals in two marine cores using principal component analysis

Jean-Pierre Valet
Institut de Physique du Globe de Paris, 1, rue Jussieu, F-75238 Paris CEDEX 05, France (valet@ipgp.jussieu.fr)

Eva Moreno
Centre de Recherches sur la Paléobiodiversité et les Paléoenvironnements, UMR 7207, Département Histoire de la Terre, Muséum National d'Histoire Naturelle, CP 48, 43, rue Buffon, F-75231 Paris CEDEX 05, France (emoreno@mnhn.fr)

Franck Bassinot
Laboratoire des Sciences du Climat et de l'Environnement, CNRS-CEA-IPSL, Domaine du CNRS, F-91198 Gif-sur-Yvette, France (bassinot@lsce.ipsl.fr)

Lola Johannes
Centre de Recherches sur la Paléobiodiversité et les Paléoenvironnements, UMR 7207, Département Histoire de la Terre, Muséum National d'Histoire Naturelle, CP 48, 43, rue Buffon, F-75231 Paris CEDEX 05, France

Fabien Dewilde
Laboratoire des Sciences du Climat et de l'Environnement, CNRS-CEA-IPSL, Domaine du CNRS, F-91198 Gif-sur-Yvette, France

Tiago Bastos, Apolline Lefort, and Marie-Thérèse Venec-Peyre
Centre de Recherches sur la Paléobiodiversité et les Paléoenvironnements, UMR 7207, Département Histoire de la Terre, Muséum National d'Histoire Naturelle, CP 48, 43, rue Buffon, F-75231 Paris CEDEX 05, France

[1] High resolution measurements of climatic and magnetic parameters have been performed on two cores from the eastern China Sea and the western Caroline Basin. On both cores, magnetic parameters show a strong imprint of climatic changes but the absence of relationship between the inclination and the bulk density indicates that the directional changes do not depend on lithology. A weak 100 ka cycle is present in the China sea inclination variations, but this period is not in phase with the orbital eccentricity and thus not relevant. All normalization parameters yielded similar estimates of relative paleointensity (RPI), but we have noticed the persistence of climatic components in the signal. Principal Component Analysis (PCA) applied to different parameters related to climate, lithology and paleointensity has allowed to extract a "clean" magnetic signal that we refer as "principal component of paleointensity (PCP)" which is in better agreement with the Sint-2000 composite curve and provides a reliable record of relative paleointensity. The presence of climatic frequencies in RPIs most likely reflects the influence of lithology on the response of magnetization to field intensity. We suggest that PCA analysis can be very useful to approach these problems. Not only can the calculation separate overlapping climatic and magnetic signals, but it indicates what confidence should be given to the data. Incidentally, the present results emphasize the importance of carrying out detailed paleoclimatic analyses along with paleointensity studies.

Components: 10,500 words, 14 figures, 2 tables.

Keywords: magnetization; paleointensity; paleomagnetism; sediments.

Index Terms: 1521 Geomagnetism and Paleomagnetism: Paleointensity; 1522 Geomagnetism and Paleomagnetism: Paleomagnetic secular variation; 1540 Geomagnetism and Paleomagnetism: Rock and mineral magnetism.

Received 11 May 2011; **Revised** 11 July 2011; **Accepted** 17 July 2011; **Published** 27 August 2011.

Valet, J.-P., E. Moreno, F. Bassinot, L. Johannes, F. Dewilde, T. Bastos, A. Lefort, and M.-T. Venec-Peyre (2011), Isolating climatic and paleomagnetic imbricated signals in two marine cores using principal component analysis, *Geochem. Geophys. Geosyst.*, *12*, Q08012, doi:10.1029/2011GC003697.

1. Introduction

[2] It has frequently been assumed that the Earth's magnetic field could be modulated by the orbital variations of the Earth's rotation axis [*Malkus*, 1968; *Kerswell*, 1996; *Vanyo and Dunn*, 2000; *Christensen and Tilgner*, 2004; *Tilgner*, 2005, 2007; *Wu and Roberts*, 2008]. Initially defended on the basis of theoretical arguments, this controversial hypothesis [*Loper*, 1975; *Rochester et al.*, 1975; *Kent and Carlut*, 2001; *Roberts et al.*, 2003; *Xuan and Channell*, 2008a] has been reactivated by the coincidence of climatic and geomagnetic events in marine sedimentary cores as well as by several reports of covarying climatic and paleomagnetic signals [*Yamazaki*, 1999; *Yamazaki and Oda*, 2002; *Stoner et al.*, 2003; *Carcaillet et al.*, 2004; *Yamazaki and Oda*, 2005; *Fuller*, 2006; *Thouveny et al.*, 2008]. Magnetic and climatic changes (mostly derived from marine $\delta^{18}O$ records) often display similar time constants, which considerably increases the difficulties for detecting whether long-term changes of the Earth's orbit can effectively exert an influence on the field, or if those apparent correlations would not result from sedimentation and magnetization processes which generate changes in various parameters like blocking functions, grain sizes [*Guyodo and Valet*, 1999; *Valet*, 2003; *Xuan and Channell*, 2008b] and other ones. Complications are enhanced by the fact that the field intensity variations are extracted after proper normalization of the magnetization intensity with respect to the amount of magnetic material, which in turn is controlled by climate. Similarly, we cannot exclude that changes in lithology and/or grain sizes could be generated by depth varying processes with possible influence on the recording of the inclination through differential compaction or subtle chemical changes [*Tauxe*, 1993; *Lund and Keigwin*, 1994; *Kodama and Davi*, 1995; *Valet*, 2003]. Overall, the signal of Natural Remanent Magnetization (NRM) is likely to be affected by changes in magnetic mineralogy, granulometry and concentration that are driven by climatic and environmental conditions. The matter is even more complicated when considering uncertainties regarding the time lag between sediment deposition and acquisition of magnetization.

[3] Various studies have been focused on the spectral contents of paleointensity and paleoclimatic signals [*Meynadier et al.*, 1992; *Tauxe and Shackleton*, 1994; *Channell et al.*, 1998; *Chapman and Shackleton*, 1999; *Channell and Kleiven*, 2000; *Guyodo et al.*, 2000; *Heslop*, 2007; *Yokoyama et al.*, 2007; *Saracco et al.*, 2009]. Other approaches have been attempted to correct the signals of relative paleointensity from changes in sediment composition [*Franke et al.*, 2004; *Hofmann and Fabian*, 2009]. However, the climatic and magnetic indicators are frequently not measured on the same cores making it difficult to establish the actual relationship between the two signals. In order to address this issue we have performed high-resolution magnetic and climatic studies from two marine cores characterized by different environmental conditions. We propose a simple technique based on principal component analysis in order to extract the part due to climatic "contamination" from the geomagnetic signal.

2. Core Locations and Oceanographic Setting

[4] The giant piston cores MD98-2182 and MD98-2194 and were retrieved during IPHIS-II cruise (IMAGES-IV) of the French R/V Marion Dufresne in 1998.

[5] Core MD98-2182 (3°31′N; 132°11′E; 37.2 m) was collected in the West Caroline Basin at the North of New Guinea, at 3575 m of water depth

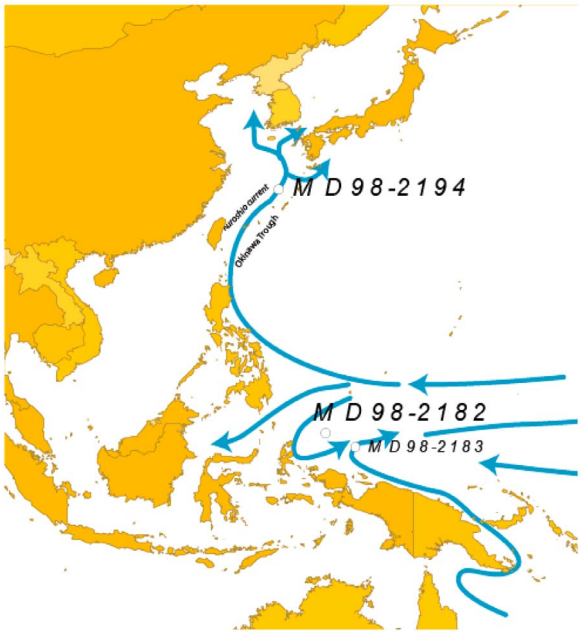

Figure 1. Core locations in the China Sea and Caroline basin.

(Figure 1). The west Caroline Basin (WCB) is located within the Western Pacific Warm Pool (WPWP), which is characterized by the largest single expanse of warm water (>28°C) and is a major source of global latent heat to the atmosphere [*Yan et al.*, 1992]. The sediment is composed of clay-rich calcareous ooze. This core is characterized by the existence of ash layers and turbidites composed of foraminifera sand levels with carbonate content up to 90%. They are easily recognized from their physical properties (p wave velocity, density, lightness) and do not exceed a few centimeters in thickness, except a 3 m thick layer at 27 m downcore. Turbidites are instantaneous deposits that are associated with important reworking of older material. Consequently, the intervals containing these layers have not been integrated and the depth scale corrected accordingly. After correction the core length was of 31.3 m for core MD98-2182 and 25 m for core MD982194.

[6] The choice of core MD98-2182 was also guided by the existence of previous magnetic studies in the same area involving cores MD98-2183, MD98-2185 and MD98-2187 [*Yokoyama and Yamazaki*, 2000; *Yamazaki and Oda*, 2002; *Yamazaki and Oda*, 2004; *Yamazaki and Oda*, 2005; *Yokoyama et al.*, 2007]. A major characteristic reported from these measurements is the existence of a 100 ka periodicity in the inclination and intensity signals persisting over the last 2.5 Myr. These cores have been collected close to or below the carbonate compensation depth. Therefore, no $\delta^{18}O$ stratigraphy was available and the age model relied on the correlation of the paleointensity records to the Sint-800 global paleointensity stack [*Guyodo and Valet*, 1999]. Detailed isotopic and magnetic records in the same cores are evidently critical to clarify the link between the climatic and magnetic variations. For this reason, a great attention was paid at obtaining high-resolution $\delta^{18}O$ records from the two present cores, which have the advantage of containing well preserved foraminifera. The present study is aimed, therefore, at analyzing high resolution climatic and magnetic variations in these two sedimentary records and discuss whether, and how, it is possible to eliminate climatic-related biases on the reconstructed field intensity variations, in order to confidently study a potential causal correlation between orbitally driven long-term climatic and geomagnetic changes.

[7] Core MD98-2194 (28°06′N–127°22′E; 29.8 m) was collected in the Okinawa trough (989 m water depth) on the oriental part of the East China Sea (Figure 1). The sediment is a clay-rich, hemipelagic ooze, fairly homogeneous in color. A dominant characteristic is the existence of several 10 cm to 170 cm thick ash layers and turbidites, which correspond to well-defined intervals of high P wave velocity that have been identified using the GEOTEK MultiSensor Track system.

3. Isotopic Measurements and Age Model

[8] Specimens containing 20 cc of sediment have been taken every 10 cm for stable oxygen isotopic stratigraphy. The samples were sieved on a 150 μm mesh sieve to retrieve planktonic foraminifera shells. Between 6 and 20 shells of the surface dwelling species Globigerinoides ruber (white, s.s.) were picked in the size fraction 250–315 μm from each sample. Shells were ultrasonically cleaned to remove clay and other impurities, and then roasted at 380°C for 40 mn in order to eliminate the organic matter. Stable oxygen isotopic compositions were measured on a Finnigan-DeltaPlus dual-inlet gas mass spectrometer. All results are expressed as $\delta^{18}O$ versus V-PDB (in ‰) with respect to NBS 19 and NBS 18 standards. The internal analytical reproducibility determined from replicate measurements of a carbonate standard is +/−0.05% (1s). The $\delta^{18}O$ records are plotted in Figure 2 for each core as a function of depth. The age models have

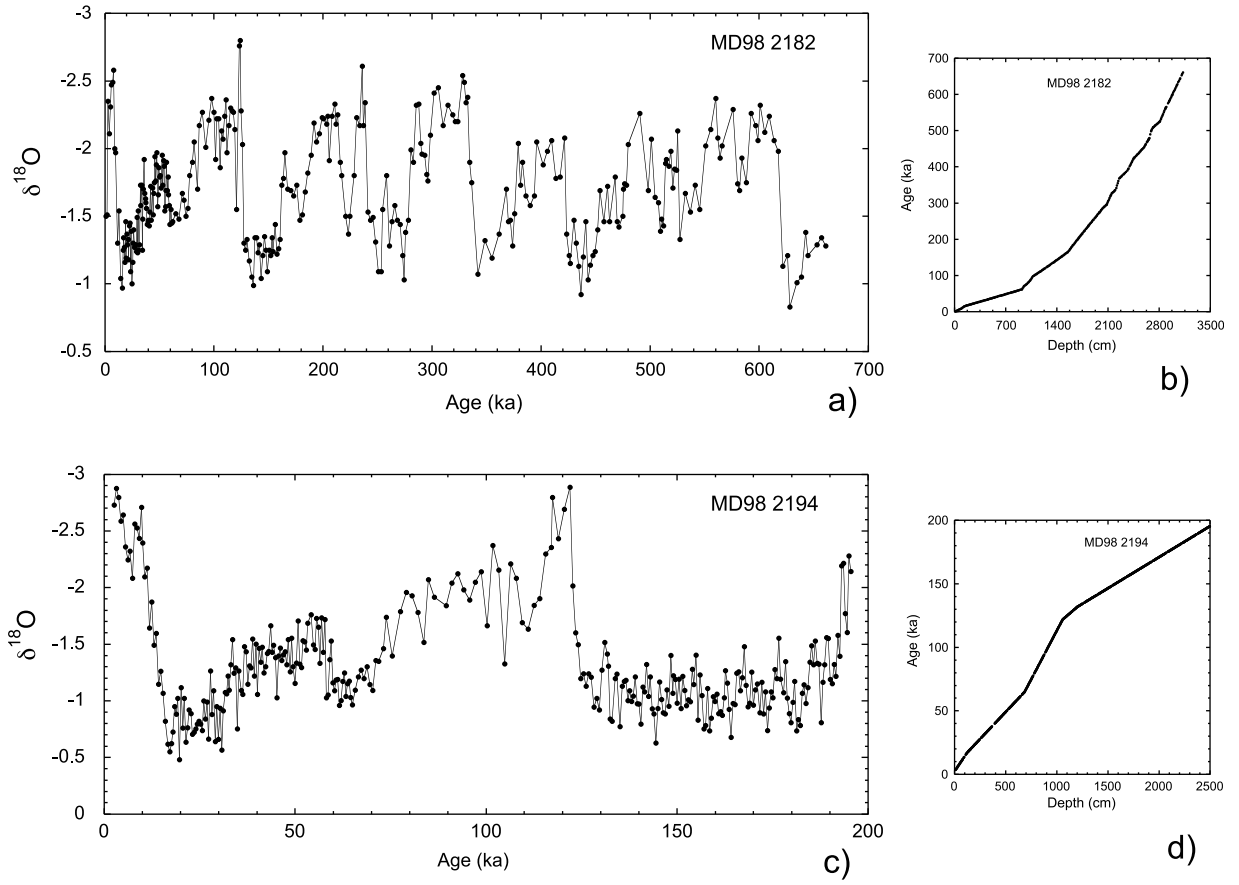

Figure 2. Evolution of the $^{18}O/^{16}O$ ratio as a function of age for (a) core MD98-2182 and (c) core MD98-2194. (b and d) Depth versus time plots showing the evolution of the deposition rates constrained by the tie points derived from the correlation with the reference curve of *Bassinot et al.* [1994].

been obtained by correlating first the G. ruber $\delta^{18}O$ records to the low-latitude, oxygen isotope stack from *Bassinot et al.* [1994], and by adjusting the final age models by fine tuning several isotopic features to the well-dated, planktonic isotopic record from Core MD98-2165 located in the Indonesian archipelago [*Waelbroeck et al.*, 2006; *Levi et al.*, 2007].

[9] The record from core MD98-2182 covers the last 660 ka (Figure 2a). The sedimentation rate (Figure 2b) is similar between glacial and interglacial periods (around 5 cm/ka) with the exception of the last glacial period where it reaches 20 cm/ka. The increase in sedimentation rates in the uppermost part of the core chiefly reflects an oversampling of sediment during the coring process, which roughly affects the upper 10 m (~the last 100 ka). Oversampling is due to the elastic rebound of the core cable that occurs just after the corer triggering, while the core barrel penetrates the upper meters of sediment. The elastic rebound results in an upward movement of the piston forcing sediments to penetrate the core barrel in excess [*Széréméta et al.*, 2004]. A similar oversampling effect has been reported for the upper part of cores MD98-2183, MD98-2185 and MD98-2187 collected in the West Caroline Basin [*Yamazaki and Oda*, 2004]. The oversampled interval has not been considered in the present study.

[10] Core MD98-2194 covers the last ~190 ka, the transition between the marine isotopic stage (MIS) 6 and 7 being reached at the bottom of the core (Figure 2c). The time versus depth plot in Figure 2d indicates relatively high deposition rates all over the 190 ka covered by the cored sediment. Sediment oversampling has not been evidenced on this core, presumably because of the shallow water depth (<1000 m), which limited the elastic rebound of the corer cable and its effects on the vertical displacement of the piston. Lower accumulation rates

prevail (<10 cm/ka) during interglacials (7.6 cm/ka for the Holocene and 7.5 cm/ka for MIS 5) and faster sedimentation prevails during glacial stages (13.8 cm/ka for the MIS 2–4 interval, and 25.4 cm/ka for MIS 6). The fast glacial accumulation of sediment was likely caused by a high input of terrigenous sediments from the Chinese continent shelf during low sea level stands. Areas of reduced deposition up the continental shelf, basinward displacement of the shoreline and the glacial river mouths induced a strong transfer of detrital material to the coring site. Note that the lower part of core MD98-2194 is characterized by a much higher accumulation rate (25.4 cm/ka).

4. Magnetic Mineralogy and Concentration

4.1. Core MD98-2182 (West Caroline Basin)

[11] Low-field magnetic susceptibility (k) was measured for all samples using a Bartington MS2 magnetic susceptibility meter. Anhysteretic remanent magnetization (ARM) was imparted in the alternating field (af) produced in the nested coils in line with the 2G magnetometer housed in the shielded room of CEREGE and IPGP. We used a peak af value of 100 mT in presence of a 50 μT dc field. Isothermal remanent magnetization (SIRMs) was imparted up to 1T. Carbonate content was measured at 10 cm sampling interval using a carbonate bomb. Samples were dried and crushed. Then, 100 mg of powder was reacted with 1 ml of HCL 6 N within a 22.4 cm^3 reactor chamber. Pressure change associated to the CO_2 degassing was converted to $CaCO_3$ content.

[12] The downcore profiles of k, ARM and SIRM covary with the $\delta^{18}O$ isotopic record (Figure 3a). Magnetic concentration is higher during interglacial periods while extremely low values are present during glacial stages 2, 3, 4 and 6. A similar correspondence has been reported in other cores from WCB and interpreted in terms of dilution by carbonates [*Yamazaki and Oda*, 2002]. After correcting the susceptibility values from the carbonate content, the signal has remained unchanged with similar glacial/interglacial fluctuations of the same amplitude (Figure 3b). Note that this result was expected since the effect of dilution by carbonates becomes significant only for a very large variability of the carbonate content [*Meynadier et al.*, 1995; *Salomé*, 2006]. In the present situation, the amplitude of the susceptibility changes largely exceeds that of the carbonates. Therefore, changes in the amount of magnetic minerals and their relation with the succession of glacial/interglacial fluctuations cannot be linked to dilution.

[13] Relative fluctuations in magnetic grain size and mineralogy have been estimated using the ARM/K [*Banerjee et al.*, 1981; *Meynadier et al.*, 1995; *Thouveny et al.*, 2000; *Moreno et al.*, 2002; *Rousse et al.*, 2006] and the S ratio that has been derived from experiments performed in a 1T direct field and a 300 mT back field ($IRM_{-0.3}$). The S ratio (defined as $(1+IR_{0.3T}/SIRM_{1T})/2$) [*Bloemendal et al.*, 1992] is always higher than 0.9 and indicates, therefore, that the magnetization is dominantly carried by a low coercivity mineral, likely magnetite. Similarly to magnetic concentration, both ARM/K and S ratios depict glacial/interglacial fluctuations with larger magnetic grain sizes and a higher ratio of hematite/magnetite during the glacial periods (Figure 4). The rapid and large amplitude fluctuations of ARM/K during the marine isotopic stages 2 and 3 may not be fully significant as they are associated with extremely low magnetic concentration. Last, the magnetic concentration parameters and the S ratio show a long-term increasing trend with depth, which indicates an increasing amount of magnetite (ARM/K).

[14] Changes in concentration and magnetic mineralogy (Figure 4) largely depend on paleoceanographic conditions that prevailed in the basin. Hematite content in marine sediments is mostly linked to the flux of aeolian material. Its higher abundance in glacial intervals of Core MD98-2182 may suggest, therefore, that the climate was drier than today in the neighbor islands of the WCB. In addition, a large area of the Indonesian continental shelf, as well as the western part of New Guinea were exposed during glacial, low sea level stands, which generated more alteration products than today [*Kawahata et al.*, 2002] and more aeolian dust. It is likely that climatic and sea level changes were not the only factors at play and that mineralogical changes also reflect modifications in deep water conditions. The reduction of deep water ventilation during glacial periods with subsequent consequences on diagenesis may have yielded dissolution of the finest fraction of magnetite and thus coarser magnetite grain sizes with a relative increase of hematite. The higher content of magnetite during interglacials should result from increased continental alteration associated with more humid climate, more intense runoffs and, therefore, lower influence of wind-

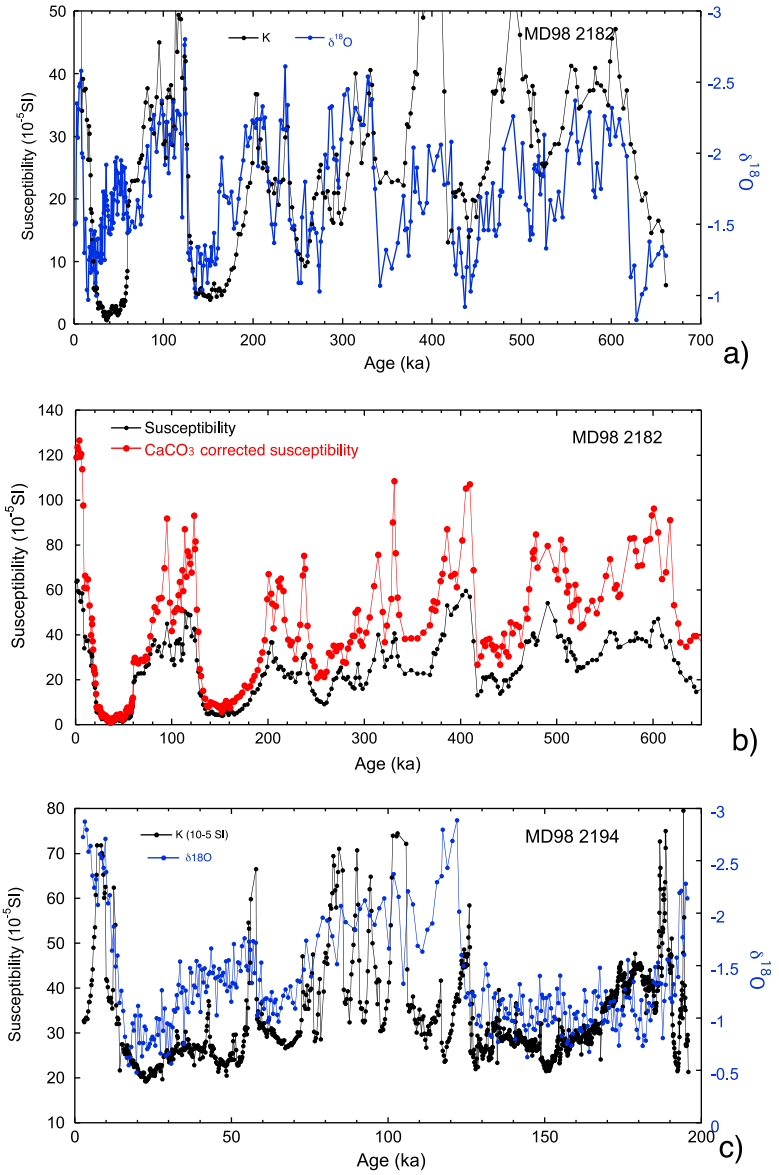

Figure 3. (a) Variations of low-field magnetic susceptibility compared with the evolution of the $\delta^{18}O/^{16}O$ ratio in core MD98-2182. (b) Variations of low-field susceptibility before and after correction from $CaCO_3$ content in core MD98-2182. (c) Same as Figure 3a but for core MD98-2194.

transported particles. In the meantime, better ventilation of deep waters and weakening of reductive diagenesis would also contribute.

4.2. East China Sea

[15] The downcore profiles of ARM and K are similar in core MD98-2194 but both show many large amplitude peaks. The most prominent spikes are present in the susceptibility record (Figures 3c and 4) at 55.3–58.2 ka (570–604 cm), 99.3–106.6 ka (908–956 cm) and 185.6–190.6 ka (2292–2398 cm) while smaller ones are associated with layers of volcanic ashes. All have been removed from the paleomagnetic record. Both parameters are not without relationship with the climatic evolution and indicate that a stronger magnetic concentration has prevailed during the interglacials. The ARM/K ratio (Figure 4) displays a similar pattern and thus reflects some coarsening of the magnetic fraction during the glacial intervals. Note also the presence of large dips which are associated with the typical large and sudden coarsening of the magnetic grain sizes within the ash layers. Two other intervals found in stages 3 (42.7–51.6 ka; 420–530 cm) and 6 (143–155 ka; 1420–

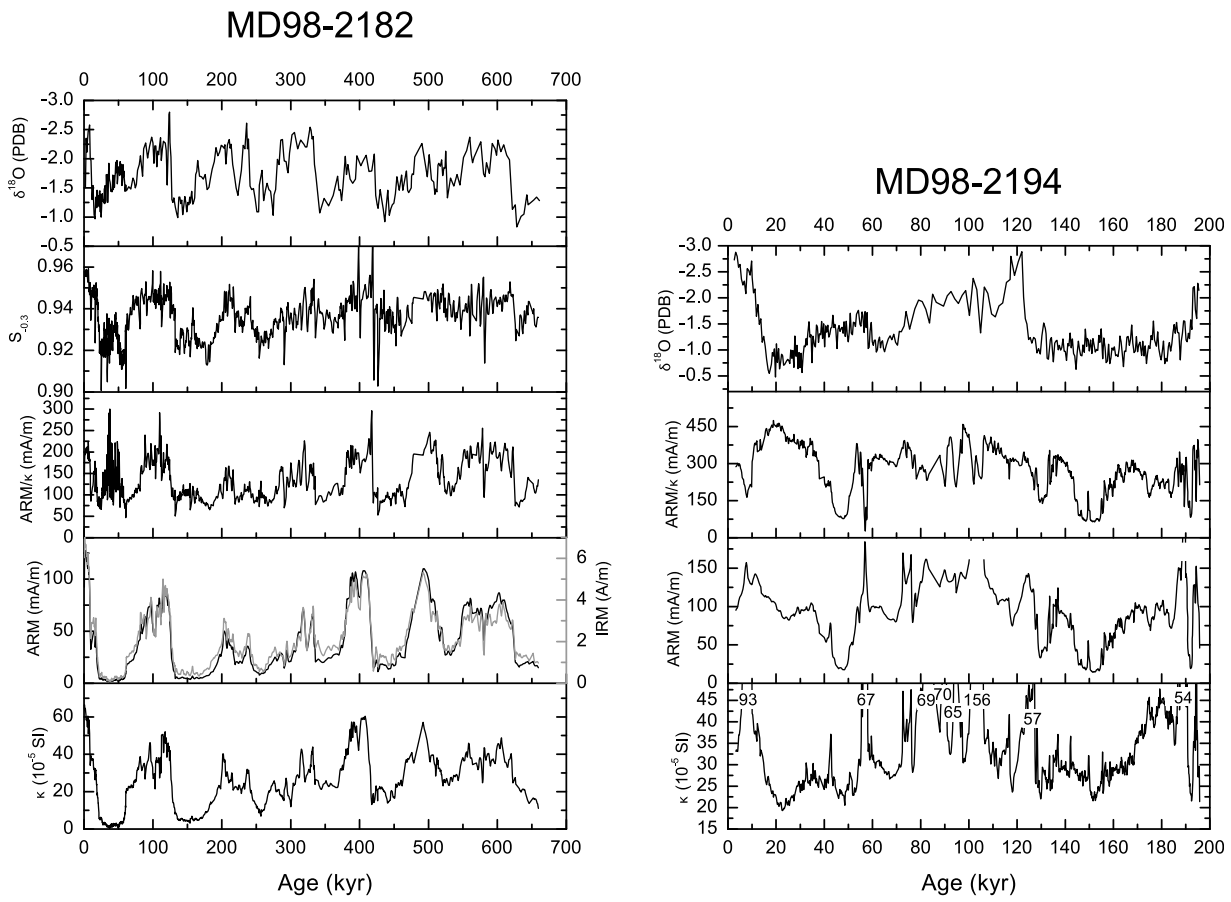

Figure 4. Rock magnetic parameters reflecting the changes in magnetic concentration, magnetic grain sizes, and magnetic mineralogy as a function of age.

1660 cm) indicate a strong coarsening of the magnetic fraction but they are not related to a specific climatic event.

5. NRM Measurements and Demagnetization

[16] The cores were sampled using 1.5 m long U channels. Measurements and stepwise demagnetization (at 5–10 mT steps up to 80 mT) have been performed every 2 cm using 2G Enterprises horizontal cryogenic magnetometers with their in line demagnetization coils in the shielded rooms of IPGP and CEREGE. Most demagnetization diagrams (Figure 5) linearly decay to the origin. In some cases, a low coercivity viscous overprint has been removed at 20 mT. The directions of the characteristic remanent magnetization (ChRM) have been derived from the best fitting line of the demagnetization diagrams passing through the origin using the PaleoMac software [*Cogné*, 2003].

[17] In the absence of core orientation the declinations plotted in Figures 6a and 6c have been corrected to provide an arbitrary zero mean declination over the time interval covered by each core. The declinations exhibit some large amplitude changes in the upper part of the cores that reflect twisting of the sediment within the core barrel. Other very small intervals with larger changes caused by clear sedimentary disturbances (i.e., turbidites) have been removed. Overall, these perturbations make the record relatively discontinuous. Due to differential rotation of some pieces of sediment within the core barrel the declinations initially retrieved in both cases displayed a complicated pattern. We have thus been constrained to reconstruct a coherent picture of the variations by matching together the successive pieces. At first, a few rotated broken blocks 0.5 to 2 m long have been assigned to the same mean declination as the layers above and below. In a second step, the declinations affected by a long wavelength torsion have been corrected using the slope of the linear

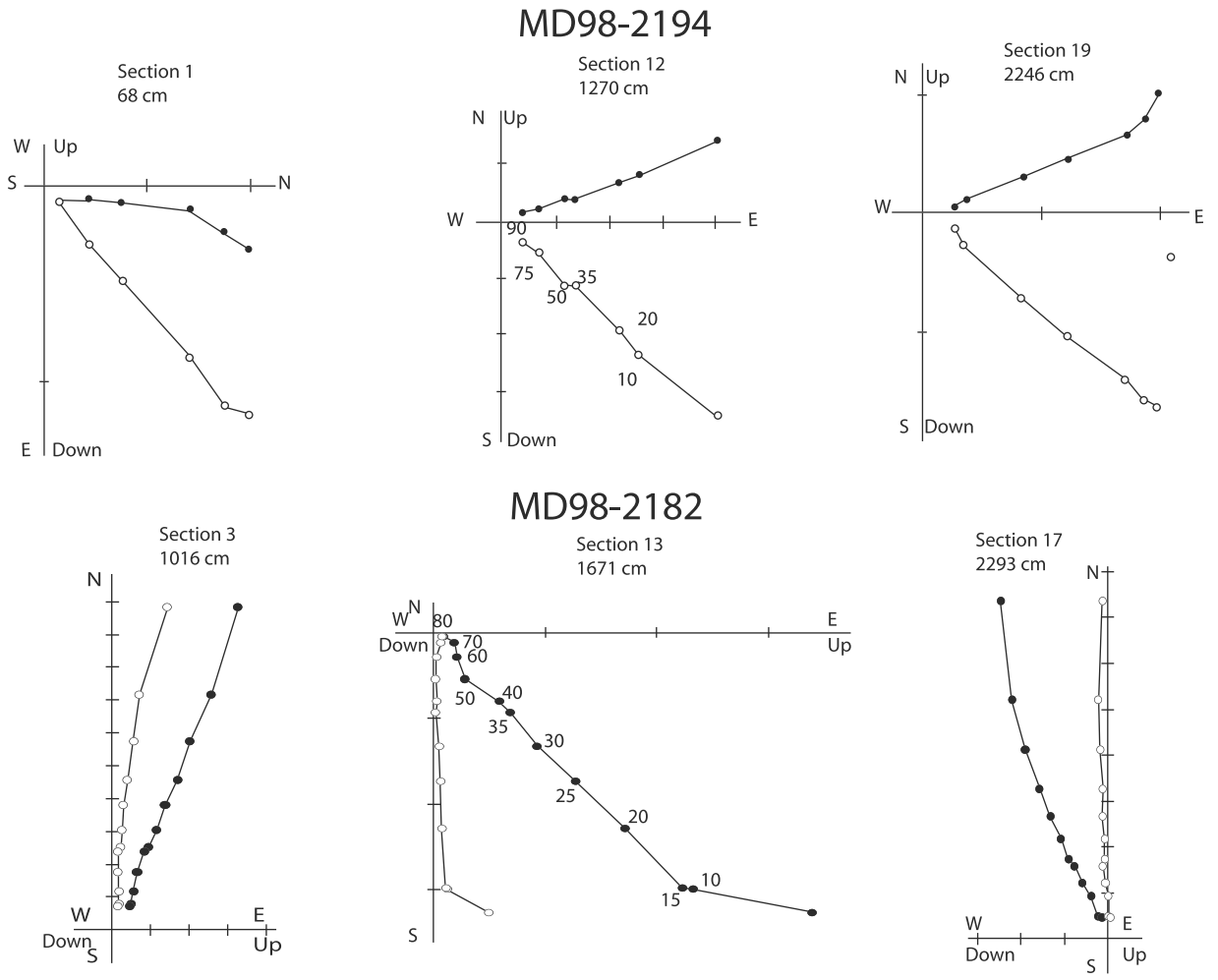

Figure 5. Typical af demagnetization diagrams from distinct stratigraphic levels in both cores.

regression between the bottom and top of the disturbed intervals. The declination records (Figures 6a and 6c) are subject, therefore, to some uncertainties, but they provide a picture of the field changes that allows us to scrutinize the occurrence of large field variations.

[18] The inclination records (Figures 6b–6d) were considerably less affected by these problems and have been plotted without any correction. The mean inclination of 44°+/−8° for core MD98-2194 (Figure 6d) is in agreement with the value of 47° expected at the coring site latitude (28°06′N). The upper 10 m from core MD98-2182 exhibit a mean inclination of 6° in perfect agreement with the geocentric axial dipole (6.5°) but with a large standard deviation of 20° likely caused by the disturbances inherent to the elongation of the sediment. Below the sediment has not been affected and the inclinations oscillate around a mean value of 0.5+/−6° which is consistent with the inclination anomaly of −6° that has been reported for the western equatorial Pacific in global models of the time-averaged field (TAF) [*Gubbins and Kelly*, 1993; *Johnson and Constable*, 1998]. Note however that this anomaly is only constrained by a few marine cores whereas volcanic data from this area are crucially needed to confirm the actual geomagnetic origin of the deviation. It has been defended [*Yamazaki et al.*, 2008] that the agreement of the mean inclinations with the predictions of the TAF models indicates the absence of inclination shallowing. However, we see here some circular reasoning since the model predictions are not validated by enough data. Interestingly, no anomaly has been reported from the paleomagnetic study conducted in a large collection of volcanic lava flows from Java [*Elmaleh et al.*, 2004].

[19] As noticed above, a striking feature of the MD98-2182 record is the large amplitude of the oscillations in the upper 8–10 m which has mainly been caused by oversampling of the water-rich

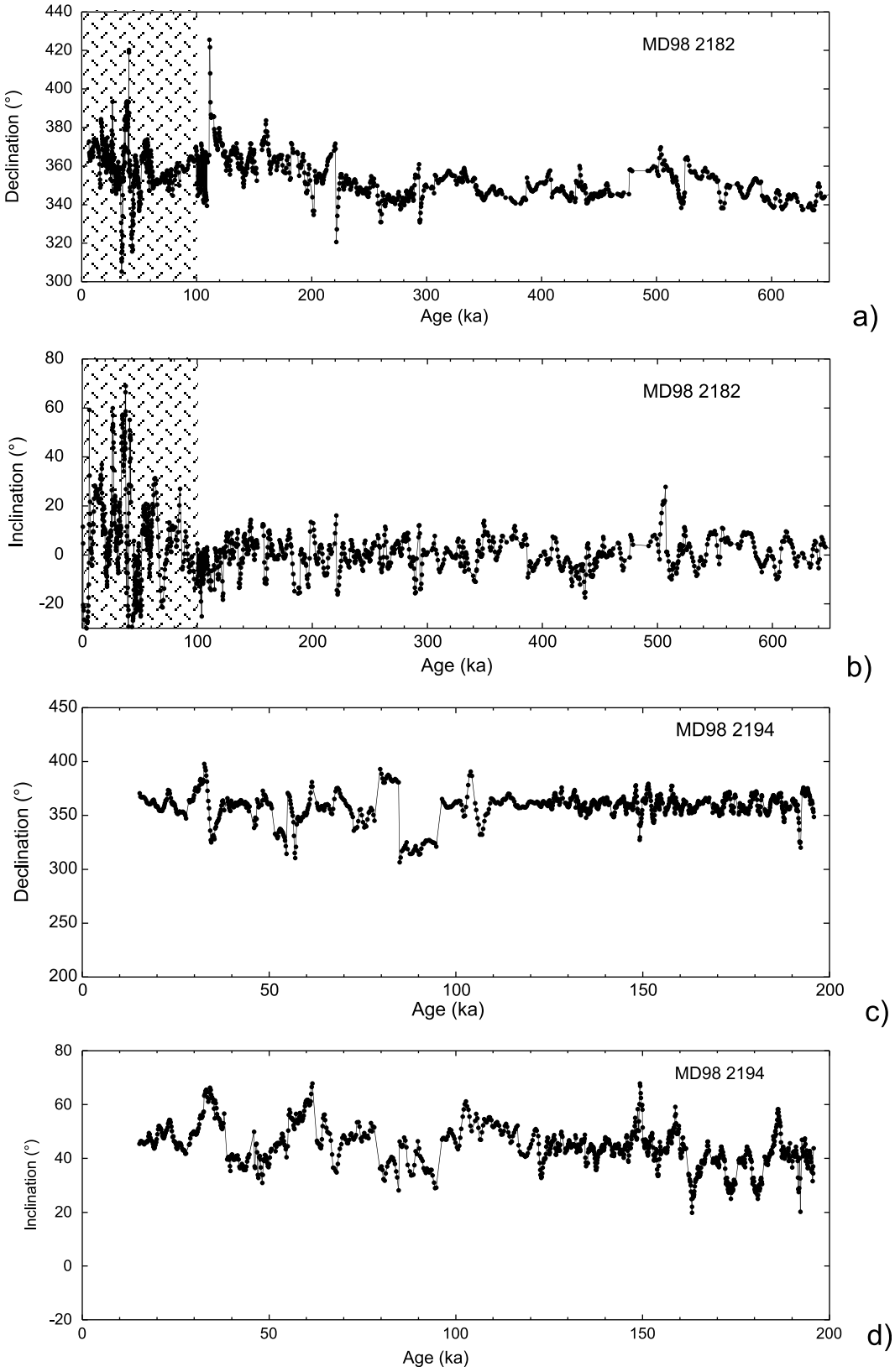

Figure 6. Declination and inclination changes for each core plotted as a function of age. The hachured intervals correspond to disturbed areas that have not been considered in the results.

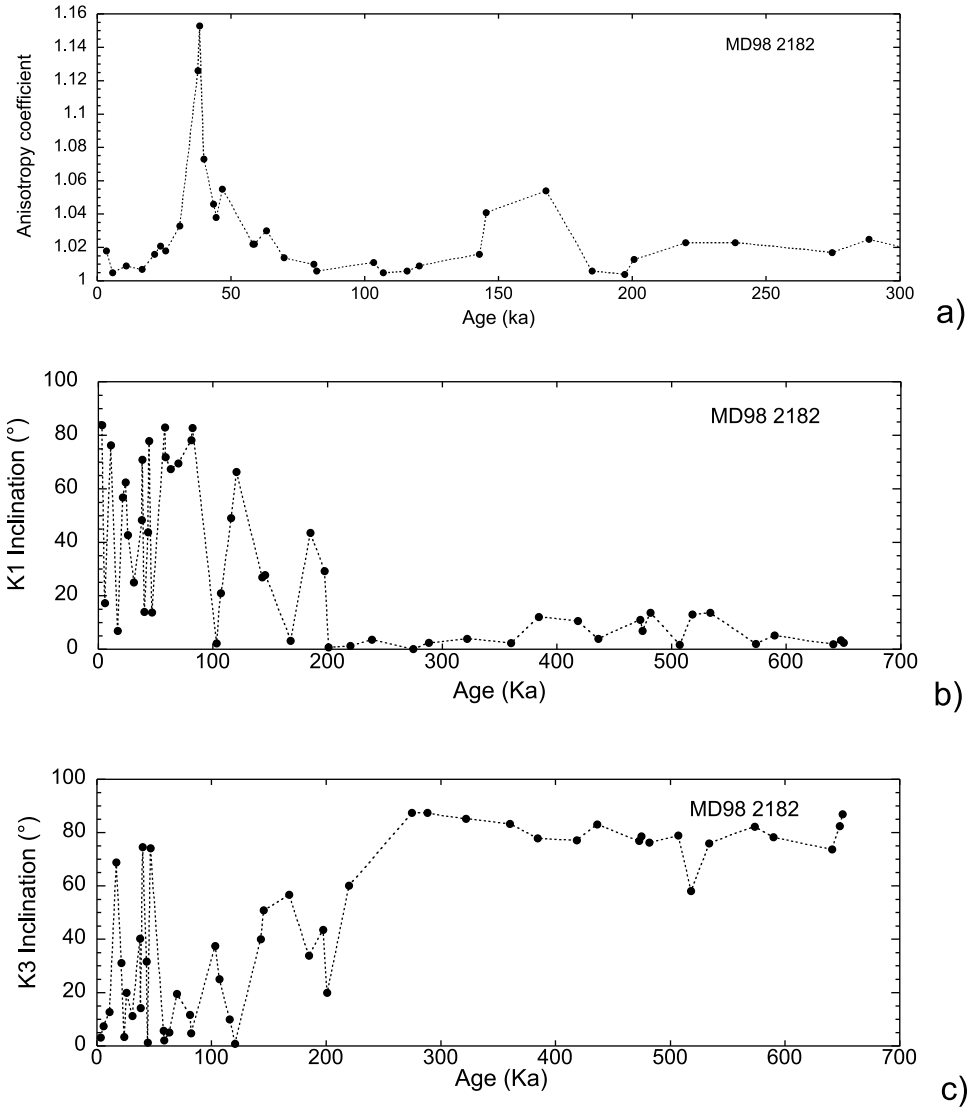

Figure 7. Parameters of magnetic anisotropy measured in core MD98-2182. The elongation of the upper part of the core is reflected by horizontal (vertical) Kmin (Kmax) axes.

upper meters of sediment within the core barrel [*Thouveny et al.*, 2000; *Skinner and McCave*, 2003; *Széréméta et al.*, 2004]. Oversampling of sediment should not be without consequences on magnetic fabric [*Thouveny et al.*, 2000]. Despite the fact that K is sensitive to coarse grains that are not involved in the remanence, we have measured the anisotropy of magnetic susceptibility. These measurements performed at deeper levels allow us to investigate whether the mean inclination has been affected by flattening caused by elongated particles lying with their long axes parallel to the horizontal plane. The mean percent of anisotropy of 1.02+/−0.03 (Figure 7a) indicates a variable elongation of the ellipsoid, which culminates at 1.15 (at about 45 ka). These observations do not really fit with the suggestion that oversampling of sediment can be accompanied by an upward elongation of the magnetic fabric. However, it is striking that the upper 100 ka are characterized by an inverse fabric with most Kmin axes (Figure 7b) lying close to the horizontal plane while the corresponding Kmax axes (Figure 7b) are characterized by very steep values. These results confirm that the magnetization of the upper 10 m of the core cannot be used with confidence.

[20] We have also scrutinized whether the inclination pattern has been influenced by differential compaction reflected by changes in the wet bulk density (WBD). Taking advantage of the high resolution measurements of WBD performed on this

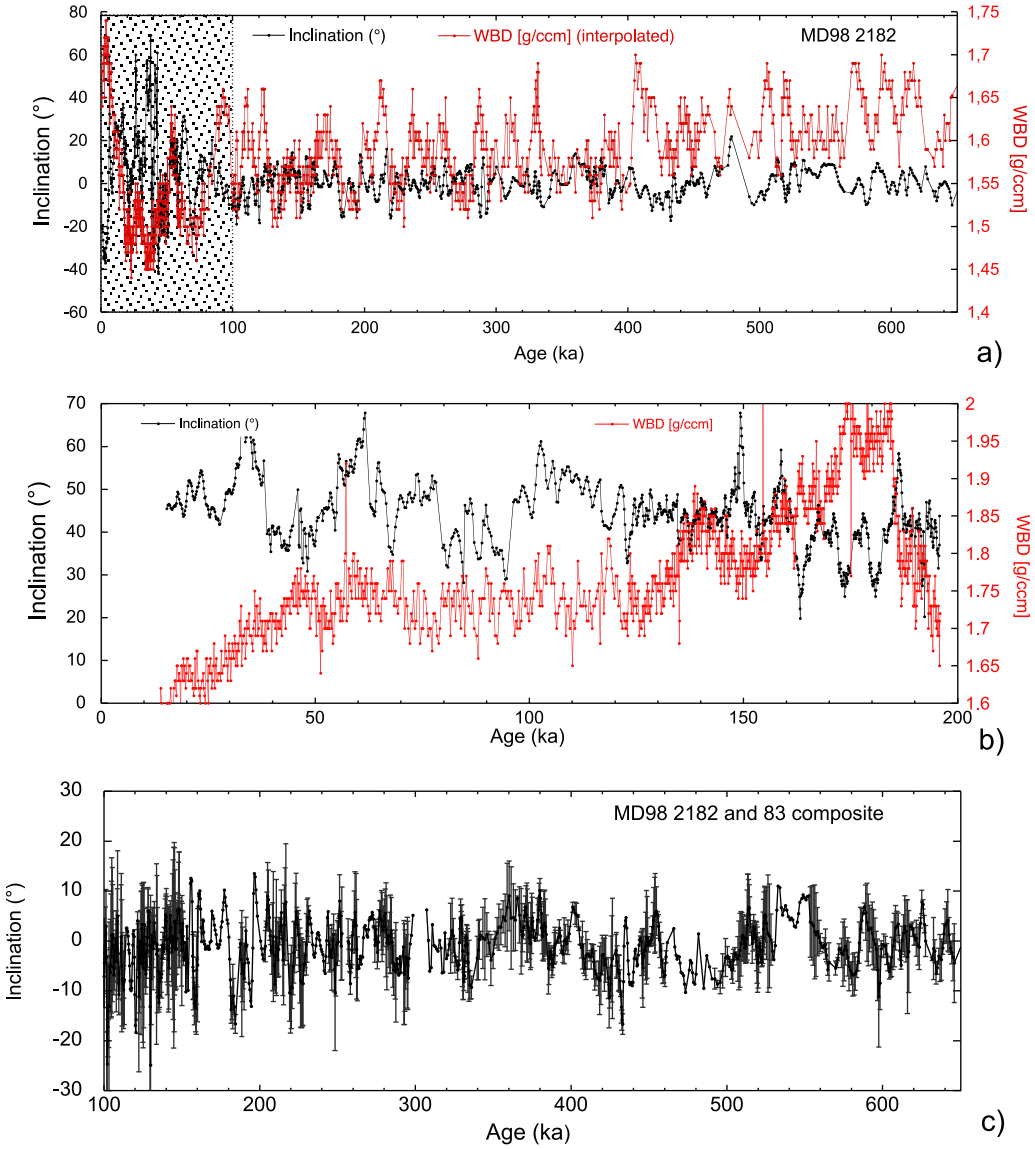

Figure 8. (a and b) Downcore variations of inclination and wet bulk density. (c) Evolution of the composite inclination derived from the variations recorded at sites 2182 and 83.

core, we can directly compare the evolution of the two parameters in Figures 8a and 8b. Despite small apparent resemblances linked to the fact that the two parameters oscillate with short wavelengths, there is no apparent relationship between the two signals. The downcore increase of density in core MD98-2194 is likely caused by compaction and has no effect on the inclination record. The next step has been to compare the present inclination record with those obtained from nearby cores that have been shown to be modulated by a 100 ka periodicity. Core MD98-2185 (3°08′N, 135°E) has been taken at about 350 km away from MD98-2182 in the same basin. Water depth at the site was 4415 m, thus below the carbonate compensation depth, so that the record has a lower resolution than core MD98-2182 and is also likely subject to uncertainties in the depth-time correlation. It is thus not surprising that the two inclination records do not perfectly match with each other. In contrast, core MD98-2183 (2°01′N, 135°02′E) located nearer core MD98-2182 is characterized by a higher resolution and by inclination changes that are similar to those of MD98-2182. Since a detailed isotopic stratigraphy has been obtained for core MD98-2182 we have relied on this suitable depth-time correspondence to combine the two inclination patterns. The agreement between the two cores was improved by matching similar features that were offset by a few ka at most. When short and large amplitude

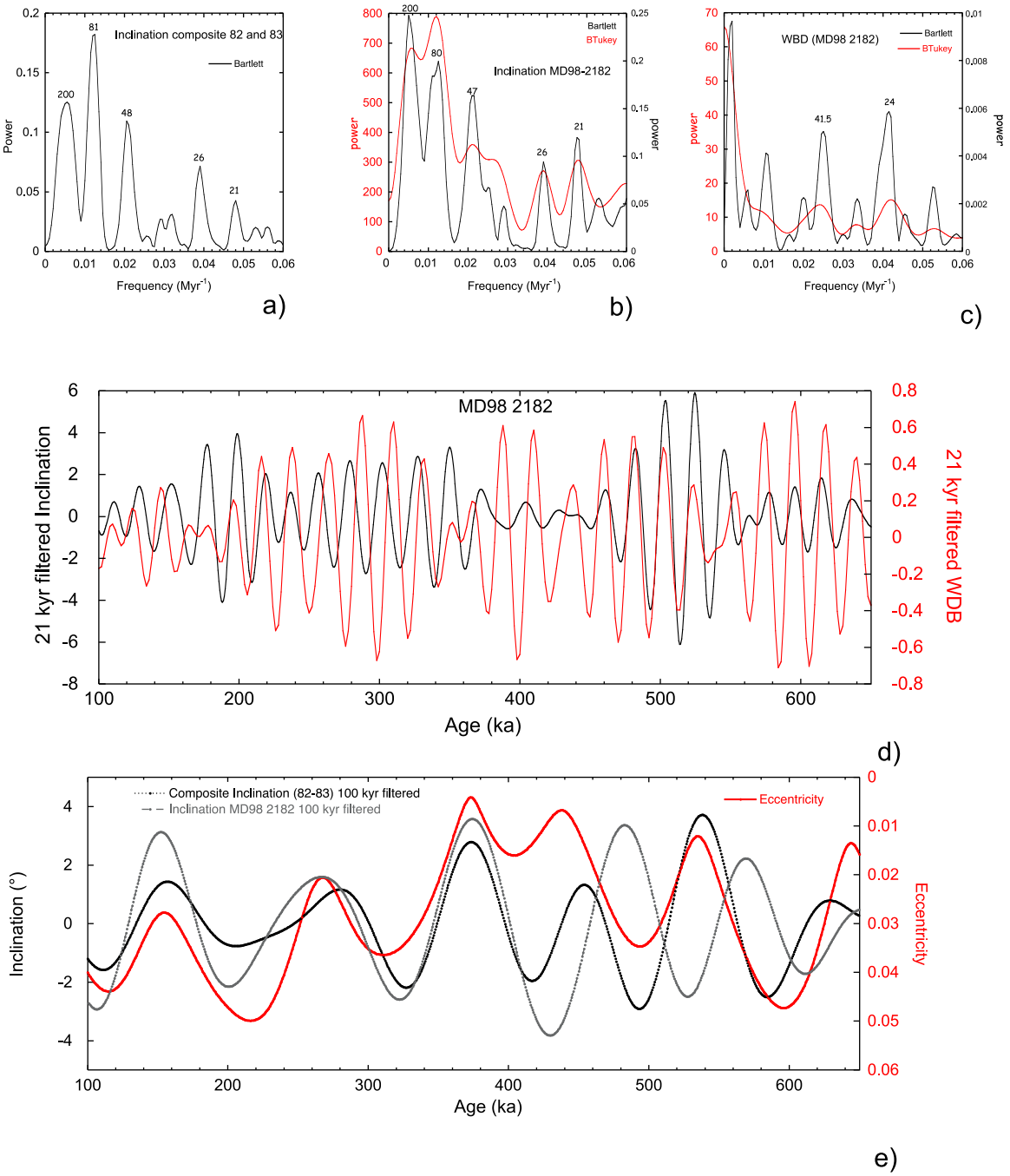

Figure 9. (a–c) Frequency spectra of the inclinations and density variations shown in Figure 8. (d) The 21 ka filtered signals of the inclination and WBD signals from core MD98-2182. (e) The 100 ka filtered signal of the inclination and the eccentricity parameter of the Earth.

deviations were present in only one record, they have been removed. The two records obtained after these little corrections are very similar. We have thus produced a composite inclination curve (Figure 8c) from these two sites, which has the advantage of removing the influence of local disturbances that can affect the amplitude of the variations.

[21] Core MD98-2182 is located in the same area as nearby cores MD98-2183 and MD98-2185 with inclination and paleointensity signals described to be modulated by a 100 ka period [*Yamazaki and Oda*, 2002; *Yokoyama et al.*, 2007]. The downcore profiles of magnetic concentration of these cores exhibit amplitude changes similar to those of

MD98-2182. However, the amplitude of their ARM/K and S ratios differ, likely as a consequence of their closer position with respect to the CCD. We expect that these small differences should not significantly affect the paleointensity records, which should all display similar periodic behavior. Spectral analyses have been applied to the inclination of core MD98-2182 (Figure 9a), to the composite inclination curve (Figure 9b) and to the WBD (Figure 9c) for the period 100–650 ka. We used the Blackman-Tukey method with two different windows (Bartlett and Tukey) in order to unambiguously identify the main frequencies without being affected by secondary peaks. Both inclination spectra are similar and point out the presence of four periods at 200, 80, 26 and 21 ka. We also note the presence of a 24 ka peak in the spectrum of the WBD. These last values may indicate some relation with the precession of the Earth's axis. We have filtered out the WBD and the inclination of MD98-2182 in order to extract the 21 ka component. The results plotted in Figure 9c show that there is no significant phase relationship between the two filtered signals. Thus, we infer that sedimentological changes and differential compaction, which are evidenced in the density variations, are not responsible for the 21 ka modulation of the inclination, but we cannot completely rule out some other complex influence associated to climatic changes. We note that the second part of the inclination record (between 400 and 650 ka) oscillates in phase with the WBD. However, because the phase relationship considerably varies with time we do not see here any causality with the climatic changes.

[22] As we have just seen above, the frequency spectra of inclination show very little evidence for a 100 ka periodicity in core MD98-2182, in contrast to the previous analyses performed from the nearby cores. The difference may be linked to the accuracy of the time scale, which in the present case has been directly established from the isotope record of MD98-2182 instead of being transferred from other records. Despite the lack of a strong signal at that periodicity in the power spectra, we have extracted the 100 ka signal from the inclination record of core MD98-2182 using a band-pass filter and then compared the variations with those of the 100 ka Earth's orbital eccentricity signal [*Laskar et al.*, 2004]. Assuming that a causal relationship would govern both signals, they should be similar or at least keep the same phase relationship. The filtered inclination signal does not keep the same phase relationship with eccentricity, particularly prior to 300 ka (Figure 9e). We infer that there is no causal relation between the two parameters.

6. Relative Paleointensity: Normalization

[23] All magnetic parameters and experiments described above have indicated that the NRM of the two cores is primarily governed by magnetite with relatively low coercivity. Magnetic homogeneity is a key factor for obtaining suitable records of relative paleointensity, otherwise the amplitude of the variations is strongly affected. The largest relative amplitude change in magnetic concentration reaches a factor 10 for core MD98-2182, which meets the current criteria of acceptance but remains quite large. Since these large changes are climatically constrained we found no reason to remove them keeping in mind the objectives of the present study. A few tiny layers from core MD98-2194 with large amplitude changes in susceptibility and likely associated to rapid sedimentation disturbances have also been removed.

[24] Before dealing with relative variations of paleointensity, attention has been paid to scrutinize the consistency of the directional changes. Since we are dealing with a full vector and not simply its modulus, the paleomagnetic directions cannot be treated independently. In the case of core MD98-2182, the existence of nearby cores was helpful for identifying critical layers with large changes that were not reproduced in all cores. Thus, we have removed the levels characterized by sudden and large variations in inclination, which cannot be related to field variations. Note that in many cases these levels are accompanied by disturbances or changes in lithology that are revealed by large variations in rock magnetic parameters, but this is not systematic. In core MD98-2194 they mostly coincide with large changes in concentration or with a few turbiditic levels.

[25] Following stepwise demagnetization of NRM, the ARM was demagnetized at the same steps of 10, 20, 30, 40, 60 and 80 mT. As expected, all demagnetization curves of ARM show a progressively linear decrease of the magnetic moment and therefore the downcore changes in the slopes fitting the NRM versus ARM plots display the same pattern as the mean NRM/ARM ratio calculated for the steps between 20 and 60 mT. These profiles are also identical to the variations derived from a single demagnetization step (e.g., NRM/ARM at 20 mT),

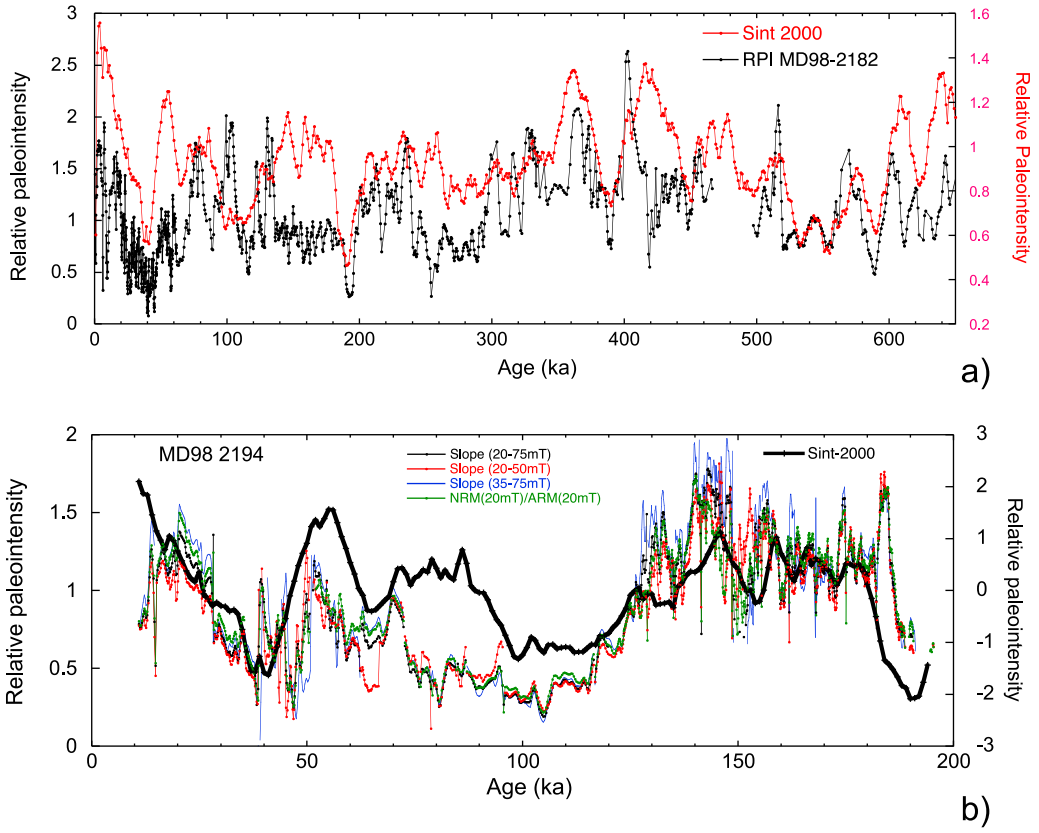

Figure 10. Records of relative paleointensity. (a) Core MD98-2182 compared with the Sint-2000 composite curve for the same period. (b) Different paleointensity proxies using various parameters for core MD98-2194 with Sint-2000.

particularly the 20 mT step which is currently selected in paleointensity studies, all viscous components being mostly removed at this stage.

[26] The standard technique for relative paleointensity (RPI) is to normalize the NRM by changes in magnetic concentration. Paleointensity records are evidently more suitable when all concentration parameters display the same downcore evolution [*Meynadier et al.*, 1992; *Valet and Herrero-Bervera*, 2000] because the relative paleointensity does not depend upon the choice of the normalizing parameter. This condition is not always taken in consideration and it happens that paleointensity records are obtained based on a single normalization parameter, usually the least sensitive to lithological changes. The profiles of NRM/K, NRM20mT/ARM20mT and NRM20mT/SIRM from core MD98-2182 have been calculated every 2 cm and they are all identical. This may be surprising given the differences between the downcore profiles of the concentration parameters. However, they are small compared to the large amplitude changes of the NRM, which governs, therefore, the ratios. The succession of the slopes derived from the NRM versus ARM demagnetization plots has also the same pattern (because of the linear decrease of ARM during demagnetization). This approach has been preferred for the record of relative paleointensity of core MD98-2182 shown in Figure 10a.

[27] The paleointensity record of core MD98-2194 from the eastern China Sea has been obtained using the arithmetic mean of the NRM/ARM and NRM/k ratios at all steps between 20 and 40 mT. The slopes fitting the plots of NRM versus ARM at different demagnetization steps display the same downcore variations as the mean NRM/ARM ratio between 20 and 60 mT (Figure 10b). These curves are also identical to the variations derived from any single demagnetization step between these two values. The NRM/K variations remain also similar to the other curves.

[28] The major problem arising from determinations of relative paleointensity is to estimate their degree of reliability. So far, despite many attempts, no parameter provides a quantitative estimate of the

quality of the records. A direct way is to compare composite curves providing that they are global and constructed from a large number of cores [*Ziegler et al.*, 2008]. Another way is to attempt corrections assuming that we are able to identify the contribution of the various factors [*Frank et al.*, 2003; *Mazaud*, 2006]. This approach has recently been followed by *Hofmann and Fabian* [2009] who corrected the records from variations of sediment composition. It relies on successive paleointensity profiles obtained by normalizing the NRM to a quantity incorporating a concentration parameter (e.g., ARM, K or SIRM) to which is added a certain amount of a "lithological" parameter. The profiles that are in closer agreement are considered as being the most reliable ones and are used, therefore, to determine the amount of lithological input that provides the optimal correction. The authors have tested the pertinence of their technique by comparing their best approximation of relative paleointensity with the Sint-800 composite record. The optimal correction has reduced discrepancies between records. A major limitation is that this approach requires multiple records. Notwithstanding we have compared proxies of relative paleointensity obtained for the two present cores using varying amounts of the normalizing parameters for core MD98-2182, but found no significant improvement in the correlation with the Sint-2000 composite curve [*Valet et al.*, 2005].

7. Principal Component Analysis

[29] The lack of successful correction may reflect the absence of linear response of the different parameters involved in the magnetization process. It is evidently reasonable to suspect that factors other than the field could affect the RPI determinations of both cores and this suspicion is likely valid for any record obtained by the current techniques for relative paleointensity. We have attempted a different approach to isolate the contributions of different components by performing principal component analyses (PCA). Not tested yet for studies of relative paleointensity, this technique uses an orthogonal transformation (derived from a set of orthogonal eigenvectors) to convert measurements of possibly correlated variables into uncorrelated variables called principal components. The first principal component has the highest variance possible and each succeeding component, in turn, has the highest remaining variance possible under the constraint that it is orthogonal to and, therefore, uncorrelated with the preceding components.

7.1. Core MD98-2182

[30] Successive calculations have been performed (using FactoMineR, an R package dedicated to multivariate Exploratory Data Analysis [*Lê et al.*, 2008]) first for three sets of parameters from core MD98-2182 that are linked to geomagnetic intensity, lithology, and climate, respectively. In this first analysis (referred to as PCA1) $\delta^{18}O$ has been used as a climatic indicator, $CaCO_3$ as a lithological indicator (which is strongly dominated by the precessional cycle) and the relative paleointensity as the geomagnetic component. In a second step (PCA2) the carbonate content has been replaced by the wet bulk density, which is mostly sensitive to lithology. Last, in PCA3 the magnetic susceptibility, which is climatically related to the changes in magnetic mineral concentration has been considered along with density and relative paleointensity (RPI). Since $\delta^{18}O$, K and WBD are all related to climate it is expected that the first and sometimes even the second principal component have a large climatic imprint. In contrast, the third component is expected to be primarily governed by the geomagnetic field without any significant climatic signature.

[31] The results of all PCA calculations performed for core MD98-2182 are given in Table 1. In Figure 11, the first and third components derived from PCA1 have been plotted along with the $\delta^{18}O$ and the paleointensity records, respectively. The PCA requires that distinct sets of measurements have been performed on the same core and, therefore, we could not apply the technique to the composite curve developed from cores MD98-2182 and MD98-2183. Table 1 gives the coefficients of linear correlation of the three principal components (Dim 1, Dim 2 and Dim 3) with the oxygen isotopes and the relative paleointensity (RPI), respectively. In all cases, the first component has extracted the climatic variations and fits very well the oxygen isotopic record. The second component (Dim 2) seems to be decoupled from the climate-related proxies and fits better the initial RPI. The third component remains correlated with climate-related proxies (except PCA3) and is in rather poor agreement with the RPI. Thus, we could argue that the second component provides the best approximation of the geomagnetic intensity. However, the coherence with the RPI is relatively meaningless since the RPI signal has not been validated as a real geomagnetic signal and may be strongly climatically contaminated. Additional complexity arises from the fact that the climatic and geomagnetic signals have similar characteristic times. We are

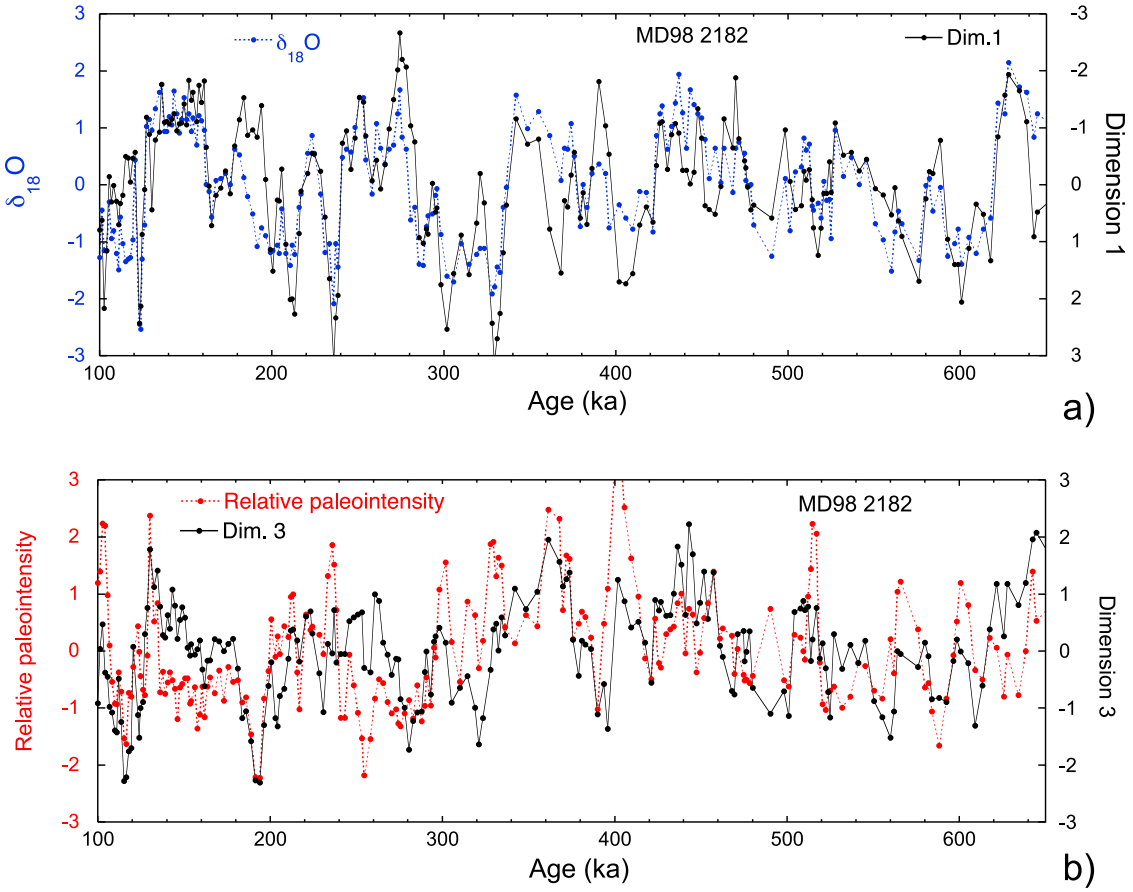

Figure 11. First and third component derived from the principal components analysis (PCA) of $\delta^{18}O$, $CaCO_3$, and RPI from core MD98-2182. (a) Dim.1 is dominated by the climatic changes as shown from comparison with the $d^{18}O/^{16}O$ changes. (b) Dim.3 has isolated the geomagnetic component which is plotted along with Sint-2000.

also aware that correlations can be limited only to specific intervals.

[32] Table 1 also gives the correlation coefficients of dim 1, dim 2 and dim 3 with the Sint-2000 record. In the present state of the art, the geomagnetic relevance of the composite curve Sint-2000 is difficult to question for several reasons. The curve integrates many cores from various paleoenvironmental conditions with different, sometimes even opposite, responses of the magnetic concentration and mineralogy to the succession of the climatic periods. It is thus reasonable to suspect that the "climatic contamination" effect has been removed. This is supported by the remarkable coherence of the Sint-2000 record with the magnetization intensity of the seafloor over the past 800 ka [*Gee et al.*,

Table 1. Results of the PCA Calculations Performed for Core MD98-2182[a]

	PCA1: $\delta^{18}O$, $CaCO_3$, RPI	PCA2: $\delta^{18}O$, WBD, RPI	PCA3: WBD, K, RPI
Dim.1/$\delta^{18}O$	0.74	0.72	0.43
Dim.1/RPI	0.60	0.54	0.64
Dim.1/Sint-2000	0.01	0.04	0.11
Dim.2/$\delta^{18}O$	0.05	0.29	0.11
Dim.2/RPI	0.66	0.84	0.70
Dim.2/Sint-2000	0.06	0.44	0.21
Dim.3/$\delta^{18}O$	0.66	0.62	0.27
Dim.3/RPI	0.48	0.1	0.33
Dim.3/Sint-2000	0.68	0.54	0.52

[a]Columns give the results of different analyses involving the parameters quoted below the PCA number. Rows show the correlation coefficients between the two parameters that are indicated in the first column. PCP/Sint = 0.68, and RPI/Sint = 0.30.

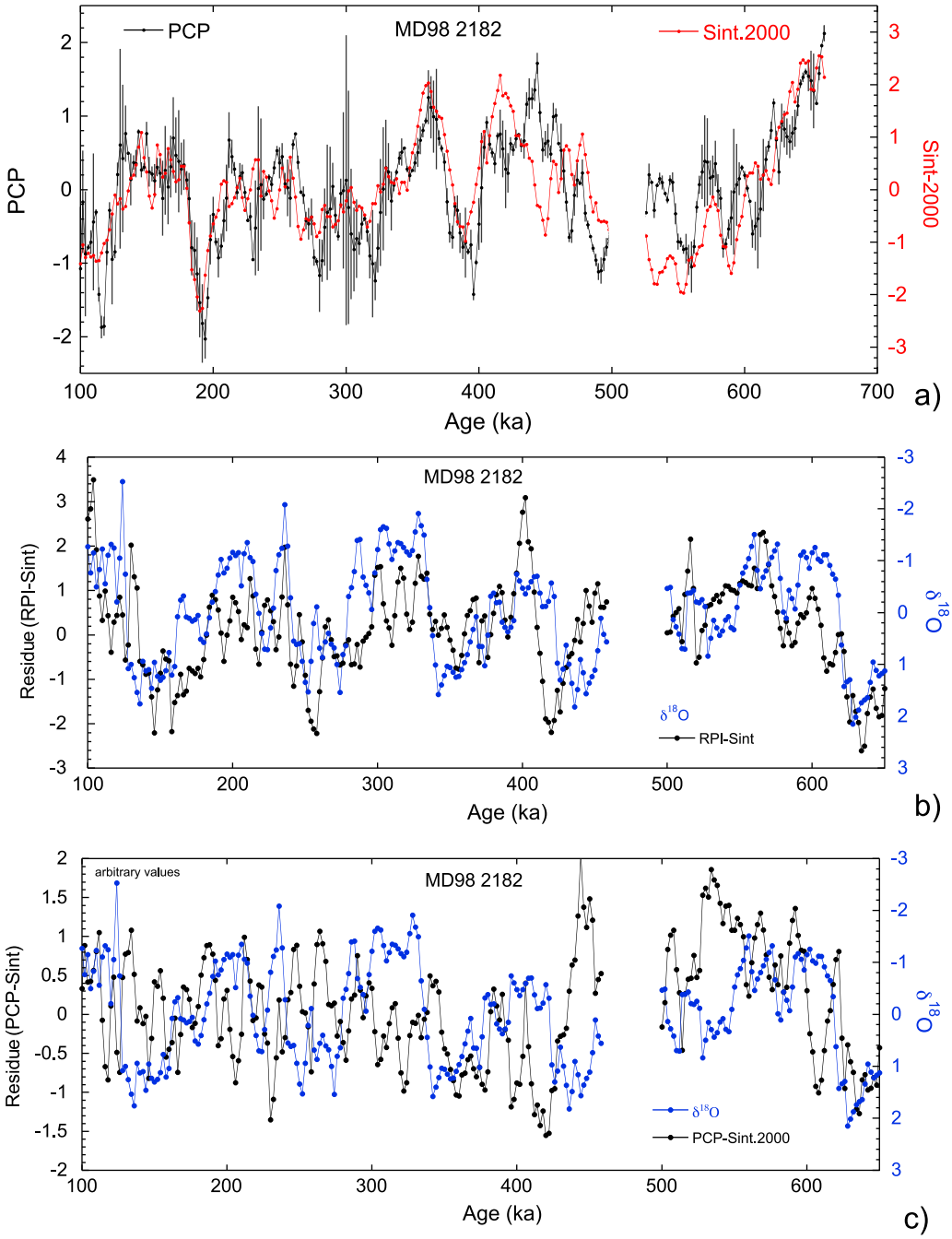

Figure 12. (a) Evolution of the principal component of paleointensity (PCP) of core MD98-2182 obtained after averaging the third component from three PCA analyses summarized in Table 1. (b) Residue between RPI and Sint-2000. (c) Residue between PCP and Sint-2000 compared with the climatic changes.

2000] as well as with the variations in production of cosmonucleides [*Baumgartner et al.*, 1998; *Carcaillet et al.*, 2003, 2004].

[33] Thus, we have relied on the respective coherence of the 3 components with Sint-2000 in order to define the most suitable field intensity estimate. In all analyses the best correlation with Sint-2000 has been obtained with the third component (PCA3), which indicates the geomagnetic origin of the signal. In order to constrain further the suitability of the determinations, all third components from the three PCAs have been stacked together into a unique curve that will be subsequently referred to as PCP for "principal component of paleointensity." In Figure 12a, we plotted the PCP along with the

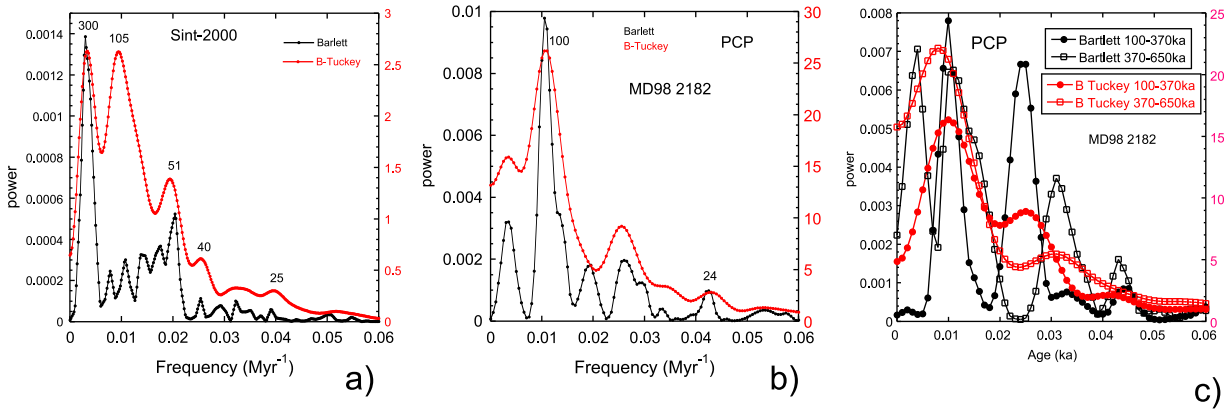

Figure 13. Frequency spectra of (a) Sint-2000 and (b) PCP. (c) Two different successive intervals of PCP.

Sint-2000 curve. The PCA approach has significantly improved the correlation ($R^2 = 0.7$) compared to that obtained with the initial RPI ($R^2 = 0.3$) and we infer that this approach has been very valuable to extract the field intensity changes from this core.

[34] In Figures 12b and 12c, we have removed the Sint-2000 geomagnetic reference curve from the paleointensity record of core MD98-2182 and from the PCP curve, respectively, both being normalized by their mean amplitude and standard deviation. Oxygen isotopes and magnetic records being measured in the same cores, we can compare the variations displayed by these two residues (Figures 12b and 12c) with the $\delta^{18}O$ record. It is striking that the residue derived from the RPI matches very well the climatic changes, particularly the fluctuations occurring on a 100 ka scale while the one obtained with the PCP does not show any striking resemblance with $\delta^{18}O$.

[35] This being said, it is puzzling that the third component has kept such a rather strong relationship with the oxygen record (Table 1). Taken at face value, this should either be interpreted as an actual causal relationship between climate and field intensity, or reflect the presence of some still unremoved imprint of lithology. In addition, we cannot rule out that different periods may have different behavior and residual paleoclimatic imprints.

[36] The first question that comes to mind concerns the spectral content of Sint-2000 (Figure 13a) and the one of the PCP (Figure 13b). Similarly to the previous analysis of inclination we used the Blackman-Tukey method with a Bartlett and a Tukey window. The PCP is characterized by a peak near 100 ka which is also present in Sint-2000 with the Bartlett window but not with the Blackman-Tukey one. Significant peaks also occur at orbital periods 41 ka and 25 ka in the PCP record which are hardly present in Sint-2000. At this stage, it is important to remind that these frequencies do not persist in Sint-2000 over the past 800 ka [*Guyodo and Valet*, 1999] and that two different spectra have been obtained when splitting the Sint-2000 record in two 400 ka long intervals (0–400 ka, 400–800 ka) and analyzing them separately. We have applied a similar approach to investigate the PCP spectrum by separating the youngest interval (100–370 ka) from the older one (370–650 ka). The very different spectra obtained for both time intervals in Figure 13c confirm the absence of stable periodicities suggesting that climatic periods are either restricted to specific intervals and/or result from combination of various frequencies.

[37] This result confirms previous studies which indicated that there is no direct physical link between paleointensity and orbital/climatic variations. The comparison between several records, including core MD98-2185 from the Caroline Basin indicates that orbital periods are significant only during limited time intervals, and these intervals are not comparable between different regions [*Xuan and Channell*, 2008b]. Similarly, *Heslop* [2007] found that cross wavelet transform analysis and squared wavelet coherence between geomagnetic records, the Sint-2000 stack [*Guyodo and Valet*, 1999; *Valet et al.*, 2005] and the marine magnetic anomaly paleointensity record [*Gee et al.*, 2000] share common power at certain orbital periods (particularly between 80 and 125 ka) with climatic records (SPECMAP stack [*Imbrie et al.*, 1993] and the ETP (Eccentricity + Tilt + Precession) curve). However, the geomagnetic and orbital variations do not exhibit a consistent phase relationship.

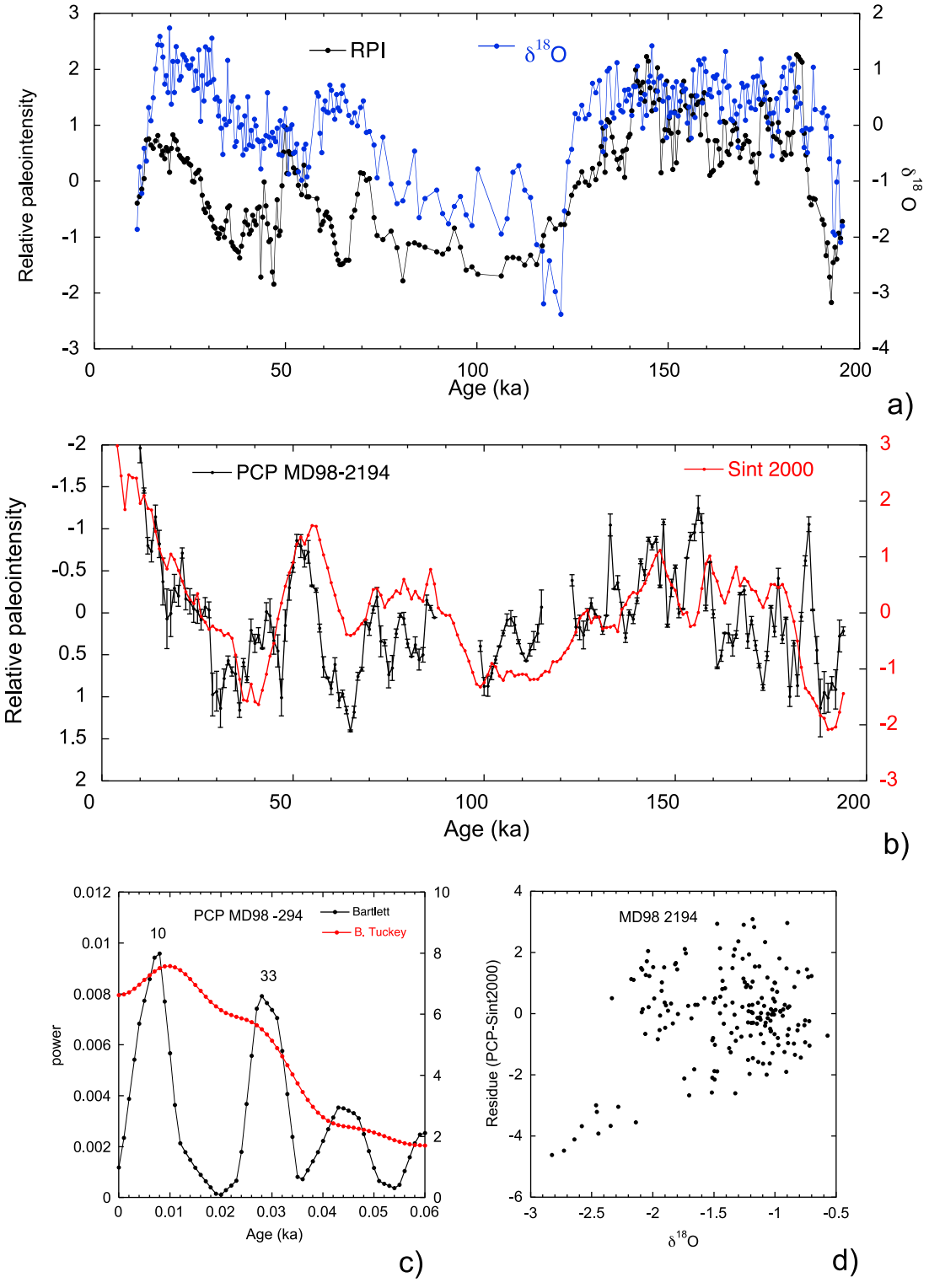

Figure 14. (a) Record of relative paleointensity of core MD98-2194 shown with its $\delta^{18}O$ variations as a function of age. (b) PCP derived from core MD98-2194 plotted for comparison with Sint-2000. (c) Frequency spectrum of PCP. (d) Residue obtained after removing PCP and Sint-2000 versus the oxygen isotopic ratio.

Table 2. Results of the PCA Calculations Performed for Core MD98-2194[a]

	PCA1: δ^{18}O, RPI, ARM, K, WBD	PCA2: δ^{18}O, RPI, WBD	PCA3: RPI, ARM, WBD
Dim.1/δ^{18}O	0.85	0.82	0.43
Dim.1/RPI	0.91	0.9	0.88
Dim.1/Sint-2000	0.04	0.03	0.07
Dim.2/δ^{18}O	0.1	0.51	0.05
Dim.2/RPI	0.0	0.08	0.06
Dim.2/Sint-2000	0.22	0.2	0.17
Dim.3–4/δ^{18}O	0.4 (dim4)	0.3	0.13
Dim.3–4/RPI	0.25 (dim4)	0.38	0.37
Dim.3/Sint-2000	0.56	0.52	0.46

[a]Same as for Table 1. PCP/Sint = 0.58, and RPI/Sint = 0.27.

7.2. Core MD98-2194

[38] The RPI and the δ^{18}O from core MD98-2194 have been plotted together in Figure 14a. There is a strong similarity between the two data sets over intervals characterized by large climatic changes, such as the onset of glacial stage 6 (~190 ka ago), the Termination II (transition from MIS 6 to MIS 5), or the Termination I (the last deglaciation, ~15 ka ago). For comparison, it is interesting to go back to Figure 10b where the paleointensity record from core MD98-2194 can be scrutinized with the Sint-2000 composite record [*Guyodo and Valet*, 1999]. The two curves show similar patterns but they are not always in phase. Some episodes such as the large decrease of the geomagnetic field surrounding the Laschamp event, 40 ka ago [*Guillou et al.*, 2004; *Plenier et al.*, 2007] are well preserved in the MD98-2194 paleointensity record. At the onset of isotopic stage 6 (about 190 ka ago), the two records display a similar rise in paleointensity although more abrupt for core MD98-2194 at the upper boundary of isotopic stage 6 (at 130 ka). Thus, the large field variations (such as the Laschamp excursion) have been correctly recorded but we cannot exclude that the RPI signal could be "contaminated" by climatic changes.

[39] Similarly to core MD98-2182, we have performed a PCA on MD98-2194 using the same succession of parameters. The correlation coefficients obtained for each component are summarized in Table 2. Again, for each PCA analysis, the climatic component appears to be dominant, while the geomagnetic component is present in the third one and even in the fourth one for the PCA first analysis. We also note that the climatic inference of component 3 is lower than for Core MD98-2182. We combined the third components of two PCA analyses (PCA1 and PCA2) to produce the PCP curve for Core MD98-2194 which has been plotted along with Sint-2000 in Figure 14b. As expected, the agreement between the two records characterized by a correlation coefficient of 0.58 is considerably higher than the value (R^2 = 0.27) that was obtained with the initial RPI. Thus, we can reasonably infer that the geomagnetic variations were better isolated by the PCA. The power spectrum (Figure 14c) of the PCP variations points out a dominant 100 ka peak, which has no significance for a 200 ka long record. The other peak at 33 ka is probably a secondary peak. This period has already been observed in some records [*Constable et al.*, 1998] and does not reflect any direct climatic or geomagnetic variable. The residue obtained after substracting Sint-2000 from the PCP is not correlated with the oxygen record (Figure 14d), suggesting that the persisting differences between the two data sets are not related to lithological changes.

8. Conclusion

[40] Different orbital frequencies have been reported by various authors who performed spectral analyses of paleomagnetic directions and paleointensity variations recorded in marine sedimentary cores. Previous studies in the Caroline basin [*Yamazaki and Oda*, 2002, 2004, 2005; *Yokoyama et al.*, 2007; *Yamazaki et al.*, 2008] have pointed out the contribution of a 100 ka periodicity in the inclination as well as in paleointensity records of several marine cores [*Thouveny et al.*, 2008]. Despite the fact that we found it conceptually difficult to imagine the physical process by which changes in the eccentricity of the Earth's orbit could influence the geodynamo, this area was appropriate for testing further the relation between the orbital parameters and the magnetization of the sediment. The present study of a nearby core (MD98-2182) has confirmed that detailed isotopic stratigraphy should ideally accompany each record of relative paleointensity, because accurate chronology is critical for analyzing the

spectral contents of the magnetic and paleomagnetic variations. Uncertainties in depth versus time correlation can rapidly yield significant differences in the frequency spectrum. In the present case, we have shown that there is no significant 100 ka periodic signal in the inclination that can be associated with the Earth's orbital frequency over the past 650 ka recorded by the sediment. Similarly, no climatic dependence could be detected in the paleomagnetic record of another core from the eastern China sea which only covers the past 200 ka but with a high deposition rate.

[41] In a second step, we have evaluated the consistency of the two records of relative paleointensity obtained by the usual normalization techniques. Despite the convergence of all techniques, we have tested whether the signal of relative paleointensity was purely geomagnetic or was altered by lithological or climatically related components. We have shown that the climatic and magnetic components could be isolated by principal component analysis providing that independent proxies linked to the climatic (e.g., $\delta^{18}O$) and lithological changes (e.g., the wet bulk density) have been documented with a good resolution. It is striking that, despite strong influence of environmental conditions, the magnetization of the two cores has preserved a geomagnetic signal which has been properly isolated in both cases, as evidenced by the comparison with the Sint-2000 composite curve. We conclude that these results point out the potential interest of PCA for studies of relative paleointensity. Alternatively, this protocol can be seen as a powerful test for evaluating the quality of the records.

Acknowledgments

[42] We are grateful to the officers, the 668 crew, and the scientists on board R/V *Marion Dufresne* for their help during the MD111-IMAGES IV cruise. Sampling of core MD98-2182 has been made possible by the MNHN Deep-Sea Sample Repository. We are grateful to M. Brunet (MNHN) and G. Isguder (LSCE) for their invaluable contributions in sample handling and preparation. We are pleased to acknowledge P.-J. Gianesinni (MNHN) for carbonate analyses. This study has been supported by the MAGORB ARN-09-BLAN0053-01 and by the French program of the MNHN Plan Pluriformation "Structure et Evolution des Ecosystèmes." This is IPGP contribution 3208 and LSCE contribution 4678.

References

Banerjee, S. K., J. King, and J. Marvin (1981), A rapid method for magnetic granulometry with applications to environmental studies, *Geophys. Res. Lett.*, *8*, 333–336, doi:10.1029/GL008i004p00333.

Bassinot, F., L. Labeyrie, E. Vincent, X. Quidelleur, N. J. Shackleton, and Y. Lancelot (1994), The astronomical theory of climate and the age of the Brunhes-Matuyama magnetic reversal, *Earth Planet. Sci. Lett.*, *126*, 91–108.

Baumgartner, S., J. Beer, J. Masarik, G. Wagner, L. Meynadier, and H. A. Synal (1998), Geomagnetic modulation of the ^{36}Cl flux in the GRIP ice core, Greenland, *Science*, *279*, 1330–1332, doi:10.1126/science.279.5355.1330.

Bloemendal, J., J. W. King, F. R. Hall, and S. J. Doh (1992), Rock magnetism of late Neogene and Pleistocene deep-sea sediments: Relation to sediment source, diagenetic processes and sediment lithology, *J. Geophys. Res.*, *97*, 4361–4375, doi:10.1029/91JB03068.

Carcaillet, J., N. Thouveny, and D. L. Bourlès (2003), Geomagnetic moment instability between 0.6 and 1.3 Ma from cosmonuclide evidence, *Geophys. Res. Lett.*, *30*(15), 1792, doi:10.1029/2003GL017550.

Carcaillet, J., D. L. Bourlès, N. Thouveny, and M. Arnold (2004), A high resolution authigenic $^{10}Be/^{9}Be$ record of geomagnetic moment variations over the last 300 ka from sedimentary cores of the Portuguese margin, *Earth Planet. Sci. Lett.*, *219*, 397–412, doi:10.1016/S0012-821X(03)00702-7.

Channell, J. E. T., and H. F. Kleiven (2000), Geomagnetic palaeointensities and astrochronological ages for the Matuyama-Brunhes boundary and the boundaries of the Jaramillo Subchron: Palaeomagnetic and oxygen isotope records from ODP Site 983, *Philos. Trans. R. Soc. London, Ser. A*, *358*, 1027–1047, doi:10.1098/rsta.2000.0572.

Channell, J. E. T., D. A. Hodell, J. McManus, and B. Lehman (1998), Orbital modulation of the Earth's magnetic field intensity, *Nature*, *394*, 464–468, doi:10.1038/28833.

Chapman, M., and N. Shackleton (1999), Global ice-volume fluctuations, North Atlantic ice-rafting events, and deep-ocean circulation changes between 130 and 70Ka, *Geology*, *27*, 795–798, doi:10.1130/0091-7613(1999)027<0795:GIVFNA>2.3.CO;2.

Christensen, U. R., and A. Tilgner (2004), Power requirement of the geodynamo from ohmic losses in numerical and laboratory dynamos, *Nature*, *429*, 169–171, doi:10.1038/nature02508.

Cogné, J. P. (2003), PaleoMac: A Macintosh™ application for treating paleomagnetic data and making plate reconstructions, *Geochem. Geophys. Geosyst.*, *4*(1), 1007, doi:10.1029/2001GC000227.

Constable, C. G., L. Tauxe, and R. L. Parker (1998), Analysis of 11 Myr of geomagnetic intensity variation, *J. Geophys. Res.*, *103*, 17,335–17,748.

Elmaleh, A., J. P. Valet, X. Quidelleur, A. Solihin, H. Bouquerel, T. Tesson, E. Mulyadi, A. Khokhlov, and A. D. Wirakusumah (2004), Palaeosecular variation in Java and Bawean Islands (Indonesia) during the Brunhes chron, *Geophys. J. Int.*, *157*, 441–454, doi:10.1111/j.1365-246X.2004.02197.x.

Frank, U., M. J. Schwab, and J. F. W. Negendank (2003), Results of rock magnetic investigations and relative paleointensity determinations on lacustrine sediments from Birkat Ram, Golan Heights (Israel), *J. Geophys. Res.*, *108*(B8), 2379, doi:10.1029/2002JB002049.

Franke, C., D. Hofmann, and T. von Dobeneck (2004), Does lithology influence relative paleointensity records? A statistical analysis on South Atlantic pelagic sediments, *Phys. Earth Planet. Inter.*, *147*, 285–296, doi:10.1016/j.pepi.2004.07.004.

Fuller, M. (2006), Geomagnetic field intensity, excursions, reversals and the 41,000-yr obliquity signal, *Earth Planet. Sci. Lett.*, *245*, 605–615, doi:10.1016/j.epsl.2006.03.022.

Gee, J. S., S. C. Cande, J. A. Hildebrand, K. Donnelly, and R. L. Parker (2000), Geomagnetic intensity variations over the past 780 kyr obtained from near-seafloor magnetic anomalies, *Nature*, *408*, 827–832, doi:10.1038/35048513.

Gubbins, D., and P. Kelly (1993), Persistent patterns in the geomagnetic field over the past 2.5 Myr, *Nature*, *365*, 829–832, doi:10.1038/365829a0.

Guillou, H., B. S. Singer, C. Laj, C. Kissel, S. Scaillet, and B. R. Jicha (2004), On the age of the Laschamp geomagnetic excursion, *Earth Planet. Sci. Lett.*, *227*, 331–343, doi:10.1016/j.epsl.2004.09.018.

Guyodo, Y., and J.-P. Valet (1999), Global changes in geomagnetic intensity during the past 800 thousand years, *Nature*, *399*, 249–252.

Guyodo, Y., P. Gaillot, and J. E. T. Channell (2000), Wavelet analysis of relative geomagnetic paleointensity at ODP Site 983, *Earth Planet. Sci. Lett.*, *184*, 109–123, doi:10.1016/S0012-821X(00)00313-7.

Heslop, D. (2007), A wavelet investigation of possible orbital influences on past geomagnetic field intensity, *Geochem. Geophys. Geosyst.*, *8*, Q03003, doi:10.1029/2006GC001498.

Hofmann, D. I., and K. Fabian (2009), Correcting relative paleointensity records for variations in sediment composition: Results from a South Atlantic stratigraphic network, *Earth Planet. Sci. Lett.*, *284*, 34–43, doi:10.1016/j.epsl.2009.03.043.

Lê, S., J. Josse, and F. Husson (2008), FactoMineR: An R package for multivariate analysis, *J. Stat. Software*, *25*(1), 1–18.

Imbrie, J., et al. (1993), On the structure and origin of major glaciation cycles: 2. The 100.000 years cycle, *Paleoceanography*, *8*, 699–735, doi:10.1029/93PA02751.

Johnson, C. L., and C. G. Constable (1998), Persistently anomalous Pacific geomagnetic fields, *Geophys. Res. Lett.*, *25*, 1011–1014, doi:10.1029/1098GL50666.

Kawahata, H., R. Maeda, and H. Ohshima (2002), Fluctuations in terrestrial-marine environments in the western equatorial Pacific during the Late Pleistocene, *Quat. Res.*, *57*, 71–81, doi:10.1006/qres.2001.2282.

Kent, D. V., and J. Carlut (2001), A negative test of orbital control of geomagnetic reversals and excursions, *Geophys. Res. Lett.*, *28*, 3561–3564, doi:10.1029/2001GL013118.

Kerswell, R. R. (1996), Upper bounds on the energy dissipation in turbulent precession, *J. Fluid Mech.*, *321*, 335–370, doi:10.1017/S0022112096007756.

Kodama, K. P., and J. M. Davi (1995), A compaction correction for the paleomagnetism of the Cretaceous Pigeon Point formation of California, *Tectonics*, *14*, 1153–1164, doi:10.1029/95TC01648.

Laskar, J., P. Robutel, F. Joutel, M. Gastineau, A. C. M. Correia, and B. Levrard (2004), A long term numerical solution for the insolation quantities of the Earth, *Astron. Astrophys.*, *428*, 261–285, doi:10.1051/0004-6361:20041335.

Levi, C., L. Labeyrie, F. Bassinot, F. Guichard, E. Cortijo, C. Waelbroeck, N. Caillon, J. Duprat, T. de Garidel-Thoron, and H. Elderfield (2007), Low-latitude hydrological cycle and rapid climate changes during the last deglaciation, *Geochem. Geophys. Geosyst.*, *8*, Q05N12, doi:10.1029/2006GC001514.

Loper, D. E. (1975), Torque balance and energy budget for the precessionally driven dynamo, *Phys. Earth Planet. Inter.*, *11*, 43–60, doi:10.1016/0031-9201(75)90074-6.

Lund, S. P., and L. Keigwin (1994), Measurement of the degree of smoothing in sediment paleomagnetic secular variation records-an example from late Quaternary deep-sea sediments of the Bermuda rise, western North-Atlantic Ocean, *Earth Planet. Sci. Lett.*, *122*, 317–330, doi:10.1016/0012-821X(94)90005-1.

Malkus, W. V. R. (1968), Precession of the Earth as the cause of geomagnetism, *Science*, *160*, 259–264, doi:10.1126/science.160.3825.259.

Mazaud, A. (2006), A first-order correction to minimize environmental influence in sedimentary records of relative paleointensity of the geomagnetic field, *Geochem. Geophys. Geosyst.*, *7*, Q07002, doi:10.1029/2006GC001257.

Meynadier, L., J.-P. Valet, R. Weeks, N. J. Shackleton, and V. L. Hagee (1992), Relative geomagnetic intensity of the field during the last 140 ka, *Earth Planet. Sci. Lett.*, *114*, 39–57, doi:10.1016/0012-821X(92)90150-T.

Meynadier, L., J. P. Valet, and F. E. Grousset (1995), Magnetic-properties and origin of upper Quaternary sediments in the Somali Basin, Indian Ocean, *Paleoceanography*, *10*, 459–472, doi:10.1029/94PA03151.

Moreno, E., N. Thouveny, D. Delanghe, I. N. McCave, and N. J. Shackleton (2002), Climatic and oceanographic changes in the northeast Atlantic reflected by magnetic properties of sediments deposited on the Portuguese Margin during the last 340 ka, *Earth Planet. Sci. Lett.*, *202*, 465–480, doi:10.1016/S0012-821X(02)00787-2.

Plenier, G., J.-P. Valet, G. Guérin, J.-C. Lefèvre, M. LeGoff, and B. Carter-Stiglitz (2007), Origin and age of the directions recorded during the Laschamp event in the Chaîne des Puys (France), *Earth Planet. Sci. Lett.*, *259*, 414–431, doi:10.1016/j.epsl.2007.04.039.

Roberts, A. P., M. Winklhofer, W.-T. Liang, and C.-S. Horng (2003), Testing the hypothesis of orbital (eccentricity) influence on Earth's magnetic field, *Earth Planet. Sci. Lett.*, *216*, 187–192, doi:10.1016/S0012-821X(03)00480-1.

Rochester, M. G., J. A. Jacobs, D. E. Smylie, and K. F. Chong (1975), Can precession power the geomagnetic dynamo?, *Geophys. J. R. Astron. Soc.*, *43*, 661–678.

Rousse, S., C. Kissel, C. Laj, J. Eiriksson, and K. L. Knudsen (2006), Holocene centennial to millennial-scale climatic variability: Evidence from high-resolution magnetic analyses of the last 10 cal kyr off North Iceland (core MD99-2275), *Earth Planet. Sci. Lett.*, *242*, 390–405, doi:10.1016/j.epsl.2005.07.030.

Salomé, A.-L. (2006), Etude sur la variabilité de la susceptibilité magnétique: Le cycle érosion-transport-sédimentation, Ph.D. thesis, 182 pp., Inst. de Phys. du Globe de Paris, Univ. Denis Diderot-Paris VII, Paris.

Saracco, G., N. Thouveny, D. L. Bourles, and J. Carcaillet (2009), Extraction of non-continuous orbital frequencies from noisy insolation data and from palaeoproxy records of geomagnetic intensity using the phase of continuous wavelet transforms, *Geophys. J. Int.*, *176*, 767–781, doi:10.1111/j.1365-246X.2008.04057.x.

Skinner, L. C., and I. N. McCave (2003), Analysis and modelling of gravity- and piston coring based on soil mechanics, *Mar. Geol.*, *199*, 181, doi:10.1016/S0025-3227(03)00127-0.

Stoner, J. S., J. E. T. Channell, D. A. Hodell, and C. D. Charles (2003), A ~580 kyr paleomagnetic record from the sub-Antarctic South Atlantic (Ocean Drilling Program Site 1089), *J. Geophys. Res.*, *108*(B5), 2244, doi:10.1029/2001JB001390.

Széréméta, N., F. Bassinot, Y. Balut, L. D. Labeyrie, and M. Pagel (2004), Oversampling of sedimentary series collected by giant piston corer: Evidence and corrections based on 3.5 kHz chirp profiles, *Paleoceanography*, *19*, PA1005, doi:10.1029/2002PA000795.

Tauxe, L. (1993), Sedimentary records of relative paleointensity of the geomagnetic field: Theory and practice, *Rev. Geophys.*, *31*, 319–354, doi:10.1029/93RG01771.

Tauxe, L., and N. J. Shackleton (1994), Relative palaeointensity records from the Ontong-Java Plateau, *Geophys. J. Int.*, *117*, 769–782, doi:10.1111/j.1365-246X.1994.tb02469.x.

Thouveny, N., E. Moreno, D. Delanghe, L. Candon, Y. Lancelot, and N. J. Shackleton (2000), Rock magnetic detection of distal ice-rafted debris: Clue for the identification of Heinrich layers on the Portuguese margin, *Earth Planet. Sci. Lett.*, *180*, 61–75, doi:10.1016/S0012-821X(00)00155-2.

Thouveny, N., D. L. Bourlès, G. Saracco, J. T. Carcaillet, and F. Bassinot (2008), Paleoclimatic context of geomagnetic dipole lows and excursions in the Brunhes, clue for an orbital influence on the geodynamo?, *Earth Planet. Sci. Lett.*, *275*, 269–284, doi:10.1016/j.epsl.2008.08.020.

Tilgner, A. (2005), Precession driven dynamos, *Phys. Fluids*, *17*, 034104, doi:10.1063/1.1852576.

Tilgner, A. (2007), Kinematic dynamos with precession driven flow in a sphere, *Geophys. Astrophys. Fluid Dyn.*, *101*, 1–9, doi:10.1080/03091920601045324.

Valet, J.-P. (2003), Time variations in geomagnetic intensity, *Rev. Geophys.*, *41*(1), 1004, doi:10.1029/2001RG000104.

Valet, J.-P., and E. Herrero-Bervera (2000), Paleointensity experiments using alternating field demagnetization, *Earth Planet. Sci. Lett.*, *177*, 43–58, doi:10.1016/S0012-821X(00)00036-4.

Valet, J.-P., L. Meynadier, and Y. Guyodo (2005), Geomagnetic dipole strength and reversal rate over the past two million years, *Nature*, *435*, 802–805.

Vanyo, J. P., and J. R. Dunn (2000), Core precession: Flow structures and energy, *Geophys. J. Int.*, *142*, 409–425, doi:10.1046/j.1365-246x.2000.00170.x.

Waelbroeck, C., C. Levi, J. C. Duplessy, L. Labeyrie, E. Michel, E. Cortijo, F. Bassinot, and F. Guichard (2006), Distant origin of circulation changes in the Indian Ocean during the last deglaciation, *Earth Planet. Sci. Lett.*, *243*, 244–251.

Wu, C. C., and P. H. Roberts (2008), A precessionally driven dynamo in a plane layer, *Geophys. Astrophys. Fluid Dyn.*, *102*, 1–19, doi:10.1080/03091920701450333.

Xuan, C., and J. E. T. Channell (2008a), Testing the relationship between timing of geomagnetic reversals/excursions and phase of orbital cycles using circular statistics and Monte Carlo simulations, *Earth Planet. Sci. Lett.*, *268*, 245–254, doi:10.1016/j.epsl.2007.12.021.

Xuan, C., and J. E. T. Channell (2008b), Origin of orbital periods in the sedimentary relative paleointensity records, *Phys. Earth Planet. Inter.*, *169*, 140–151, doi:10.1016/j.pepi.2008.07.017.

Yamazaki, T. (1999), Relative paleointensity of the geomagnetic field during Brunhes Chron recorded in North Pacific deep-sea sediment cores: Orbital influence?, *Earth Planet. Sci. Lett.*, *169*, 23–35, doi:10.1016/S0012-821X(99)00064-3.

Yamazaki, T., and H. Oda (2002), Orbital influence on Earth's magnetic field: 100,000-year periodicity in inclination, *Science*, *295*, 2435–2438, doi:10.1126/science.1068541.

Yamazaki, T., and H. Oda (2004), Intensity-inclination correlation on long-term secular variation of the geomagnetic field and its relevance to persistent non-dipole component, in *Timescales of the Internal Geomagnetic Field*, *Geophys. Monogr. Ser.*, vol. 145, edited by J. E. T. Channell et al., pp. 287–298, AGU, Washington, D. C.

Yamazaki, T., and H. Oda (2005), A geomagnetic paleointensity stack between 0.8 and 3.0 Ma from equatorial Pacific sediment cores, *Geochem. Geophys. Geosyst.*, *6*, Q11H20, doi:10.1029/2005GC001001.

Yamazaki, T., T. Kanamatsu, S. Mizuno, N. Hokanishi, and E. Z. Gaffar (2008), Geomagnetic field variations during the last 400 kyr in the western equatorial Pacific: Paleointensity-inclination correlation revisited, *Geophys. Res. Lett.*, *35*, L20307, doi:10.1029/2008GL035373.

Yan, X. H., C. R. Ho, Q. Zheng, and V. Klemas (1992), Temperature and size variabilities of the Western Pacific Warm Pool, *Science*, *258*, 1643–1645, doi:10.1126/science.258.5088.1643.

Yokoyama, Y., and T. Yamazaki (2000), Geomagnetic paleointensity variation with a 100 kyr quasi-period, *Earth Planet. Sci. Lett.*, *181*, 7–14, doi:10.1016/S0012-821X(00)00199-0.

Yokoyama, Y., T. Yamazaki, and H. Oda (2007), Geomagnetic 100-ky variation extracted from paleointensity records of the equatorial and North Pacific sediments, *Earth Planets Space*, *59*, 795–805.

Ziegler, L., C. G. Constable, and C. L. Johnson (2008), Testing the robustness and limitations of 0.1 Ma absolute paleointensity data, *Phys. Earth Planet. Inter.*, *170*, 34–45, doi:10.1016/j.pepi.2008.07.027.